Accepted Manuscript

Antimicrobial and KPC/AmpC inhibitory activity of functionalized benzosiloxaboroles

Krzysztof Durka, Agnieszka E. Laudy, Łukasz Charzewski, Mateusz Urban, Karolina Stępień, Stefan Tyski, Krystiana A. Krzyśko, Sergiusz Luliński

PII: S0223-5234(19)30246-6

DOI: https://doi.org/10.1016/j.ejmech.2019.03.028

Reference: EJMECH 11198

To appear in: *European Journal of Medicinal Chemistry*

Received Date: 2 January 2019

Revised Date: 11 March 2019

Accepted Date: 12 March 2019

Please cite this article as: K. Durka, A.E. Laudy, Ł. Charzewski, M. Urban, K. Stępień, S. Tyski, K.A. Krzyśko, S. Luliński, Antimicrobial and KPC/AmpC inhibitory activity of functionalized benzosiloxaboroles, *European Journal of Medicinal Chemistry* (2019), doi: https://doi.org/10.1016/j.ejmech.2019.03.028.

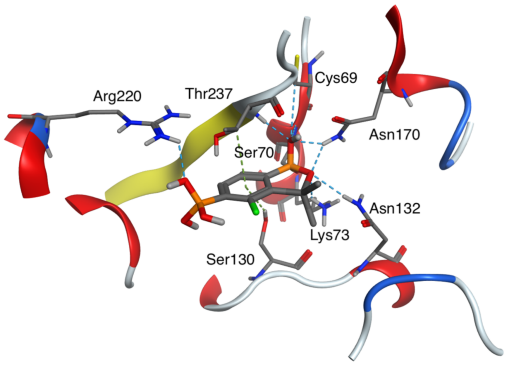

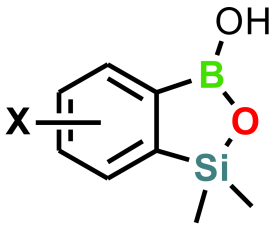

Benzosiloxaboroles

22 compounds

- KPC/AmpC enzyme inhibitory activity
- Antifungal activity
- Simple preparation

X = H, Hal (F, Cl, Br), CHO, $B(OH)_2$

Antimicrobial and KPC/AmpC inhibitory activity of functionalized benzosiloxaboroles

Krzysztof Durka,[$,a] Agnieszka E. Laudy,[$,**b] Łukasz Charzewski,[$,d] Mateusz Urban,[a] Karolina Stępień,[b] Stefan Tyski,[b,c] Krystiana A. Krzyśko,[***d] Sergiusz Luliński*[a]

[a]*Physical Chemistry Department, Faculty of Chemistry, Warsaw University of Technology, Noakowskiego 3, 00-664 Warsaw, Poland*

[b]*Department of Pharmaceutical Microbiology, Medical University of Warsaw, Oczki 3, 02-007 Warsaw, Poland*

[c]*Department of Antibiotics and Microbiology, National Medicines Institute, Chełmska 30/34, 00-725 Warsaw, Poland*

[d] *Faculty of Physics, University of Warsaw, Pasteura 5, 02-093 Warsaw, Poland*

*Corresponding author responsible for chemical research. Email address: serek@ch.pw.edu.pl (S. Luliński).

**Corresponding author responsible for microbiological research. Email address: alaudy@wp.pl (A.E. Laudy).

***Corresponding author responsible for molecular modelling. Email address: krzysko@bioexploratorium.pl (K.A. Krzyśko).

[$]These authors equally contributed to this work

Keywords: benzosiloxaboroles, antifungal activity, antibacterial activity, AmpC/KPC β-lactamase inhibitory activity, molecular docking, efflux pump

Abstract

A series of 22 benzosiloxaboroles, silicon analogues of strong antimicrobial agents - benzoxaboroles, have been synthesized and tested against β-lactamases KPC- and pAmpC-producing strains of Gram-negative rods. Comprehensive structural-property relationship studies supported by molecular modelling as well as biological studies reveal that 6-$B(OH)_2$-substituted derivative **27** strongly inhibits the activity of cephalosporinases (chromosomally encoded AmpC and plasmid encoded CMY-2) and KPC carbapenemases. It also shows strong

ability to inhibit the growth of the strains producing KPC-3 when combined with meropenem. In addition, halogen-substituted (mono-, di- or tetra-) benzosiloxaboroles demonstrate high antifungal activity (MIC 1.56-6.25 mg/L) against *C. tropicalis*, *C. guilliermondii* and *S. cerevisiae*. The highest activity against pathogenic yeasts (*C. albicans*, *C. krusei* and *C. parapsilosis* - MICs 12.5 mg/L) and against Gram-positive cocci (*S. aureus* and *E. faecalis* - 6.25 mg/L and 25 mg/L respectively) was displayed by 6,7-dichloro-substituted benzosiloxaborole. The studied systems exhibit low cytotoxity toward human lung fibroblasts.

Introduction

1,3-Dihydro-1-hydroxy-2,1-benzoxaborole and its derivatives were synthesized and characterized already in 1957 (Scheme 1) [1]. In the last decade, strong interest in these boron heterocycles was stimulated to a major extent by discovery of their biological activity [2-8]. For instance, 5-fluoro- and 5-chloro-1,3-dihydro-2,1-benzoxaborole (referred to AN2690 as tavaborole and AN2718, respectively) were identified as potent antifungal and antibacterial agents [2]. Gratifyingly, these compounds exhibit low toxicity to humans and thus the former compound has already been commercialized under trade name *Kerydin*, for treatment of onychomycosis - a fungal infection of nail and nail bed [9-10]. Very recently, 5-(4-cyanophenoxy)benzoxaborole (crisaborole, trade name *Eucrisa*) was approved for the treatment of mild-to-moderate atopic dermatitis (eczema) [11]. Other benzoxaboroles are also effective against important human diseases including malaria [12], human African trypanosomiasis (HAT) [13], and selected liver disfunctions [14]. Recently we have presented silicon-based analogues of benzoxaboroles – benzosiloxaboroles (**Scheme 1**). The electronic properties of silicon are quite different from those of carbon. Specifically, the presence of low-lying antibonding σ* orbitals at the silicon atom gives rise to significant interaction with lone pair at the adjacent oxygen atom which, in turn, results in the increased Lewis acidity of the boron atom in benzosiloxaborole compared to benzoxaborole (where the carbon atom is present instead of the silicon). In addition, the increased atomic radius of silicon results in slightly different geometry of the siloxaborole ring due to longer bonds formed by the silicon atom. Our goal was to exploit specific electronic and steric (geometric) characteristics of benzosiloxaboroles in order to obtain systems showing improved antimicrobial activity. Indeed, our preliminary microbiological studies showed their promising activity against selected yeast strains [15].

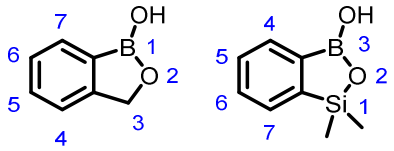

Scheme 1. Benzoxa- and benzosiloxaboroles. Position numbering scheme is additionally provided (note that it is different between benzoxa- and benzosiloxaboroles).

Herein, we report on comprehensive characterization of antimicrobial potential of 22 benzosiloxaboroles and the structure-properties relationships by varying the type, number and positions of substituents. The studied compounds can be divided into 3 subgroups. The first group comprises the parent benzosiloxaborole and its halogen (F, Cl, Br, CF_3)-substituted derivatives including two structural analogues of tavaborole (Scheme 2, **I**). This is rationalized by the fact that related benzoxaboroles containing halogen atoms located at the 4- or 5-position show enhanced antimicrobial activity. The second group contains benzosiloxaboroles bearing CHO or $B(OH)_2$ group in different configurations (**II**). We assumed that such systems might exhibit increased affinity to target biological sites due to the auxiliary interactions between an enzyme and a polar functional group. Finally, three bifunctional systems with two oxaborole rings (**III**) were studied in order to find any synergistic effects resulting from such an extended structure.

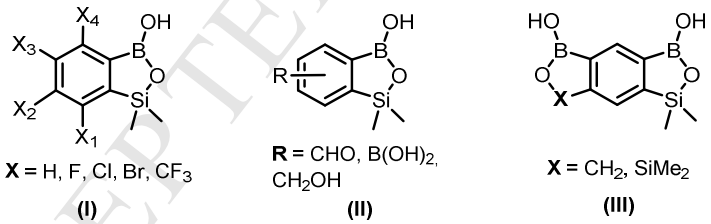

Scheme 2. Studied groups of benzosiloxaboroles.

Results and Discussion

Synthesis

The synthesis of the parent benzosiloxaborole **1** and its simple fluorinated analogues **2-4** (**Scheme 3**) was described in our seminal paper [15]. The synthesis of halogenated **10-14** (**Scheme 4**) derivatives utilizes two step protocol. Thus, appropriate halogenated bromobenzenes were subjected to deprotonative lithiation with LDA in THF at –78 °C followed by addition of $Me_2Si(H)Cl$ resulting in the formation of arylsilanes **5-8**. In all cases

reactions occurred regioselectively at the position between bromine and another halogen atom in agreement with the cumulated *ortho*-acidifying effect of those two substituents [16,17]. The silylated derivatives were successfully converted into respective benzosiloxaboroles by bromine-lithium exchange performed using *t*-BuLi at low temperatures (–75 °C) followed by trapping of generated aryllithium intermediates with an excess of $B(OMe)_3$. Final hydrolysis with dilute aqueous H_2SO_4 gave rise to targeted products with good yields. The synthesis of 6-CF_3 substituted derivative **14** utilized an analogous approach. In this case, the intermediate arylsilane **9** was obtained by regioselective deprotonation of 4-bromobenzotrifluoride with LTMP/THF at –80 °C [18].

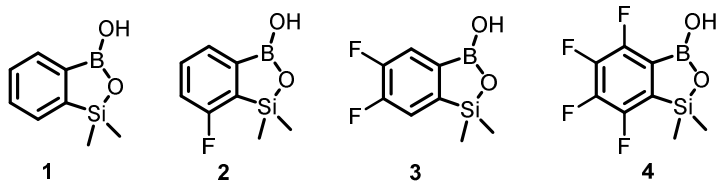

Scheme 3. Parent benzosiloxaborole and its fluorinated analogues.

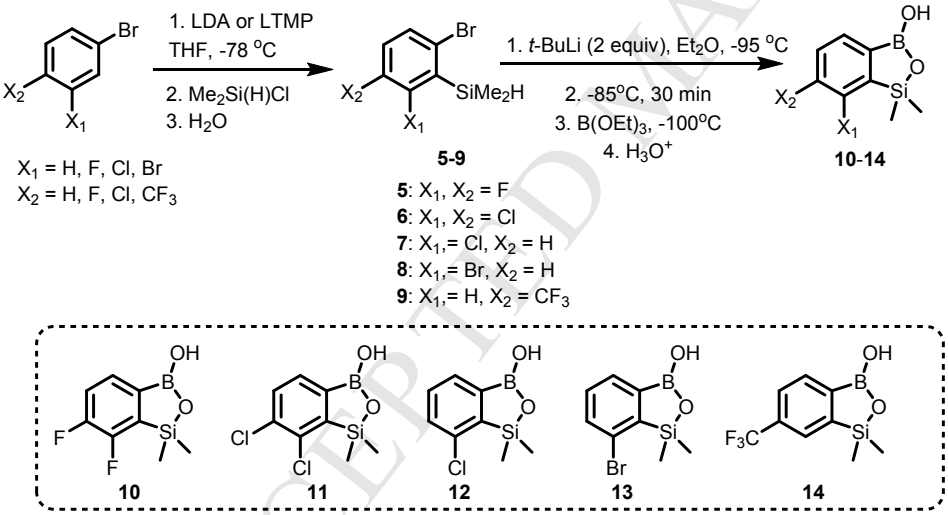

Scheme 4. Synthesis of halogenated benzosiloxaboroles **10-14**.

We were especially interested in the preparation of benzosiloxaboroles **23** and **24** as those compounds are structural analogues of tavaborole due to the presence of halogen (X = F, Cl) at the 6-position (*para* with respect to the boron atom). They were obtained in multistep protocols starting with monobromination of respective 4-haloanilines (Scheme 5) [19,20]. Subsequent replacement of amino group in **15-16** with iodine gave rise to corresponding 1-bromo-2-iodobenzenes **17-18** [21,22]. Then selective iodine-lithium exchange/in situ trapping with $B(OiPr)_3$ [23,24] was accomplished using *n*-BuLi in a mixed solvent (THF/Et_2O 1:1) at –

90 °C. The resulting respective *ate* complexes were treated with Me_3SiCl to give halogenated aryl boronates **19-20** which were further converted to dioxaazaborocans **21-22** by transesterification with *N*-butyldiethanolamine (BDEA) in Et_2O. Finally, compounds **21-22** were subjected to bromine-lithium exchange with *n*-BuLi in THF and the generated aryllithium intermediates were trapped with $Me_2Si(H)Cl$. Hydrolysis with dilute aqueous H_2SO_4 resulted in the formation of targeted products **23-24**.

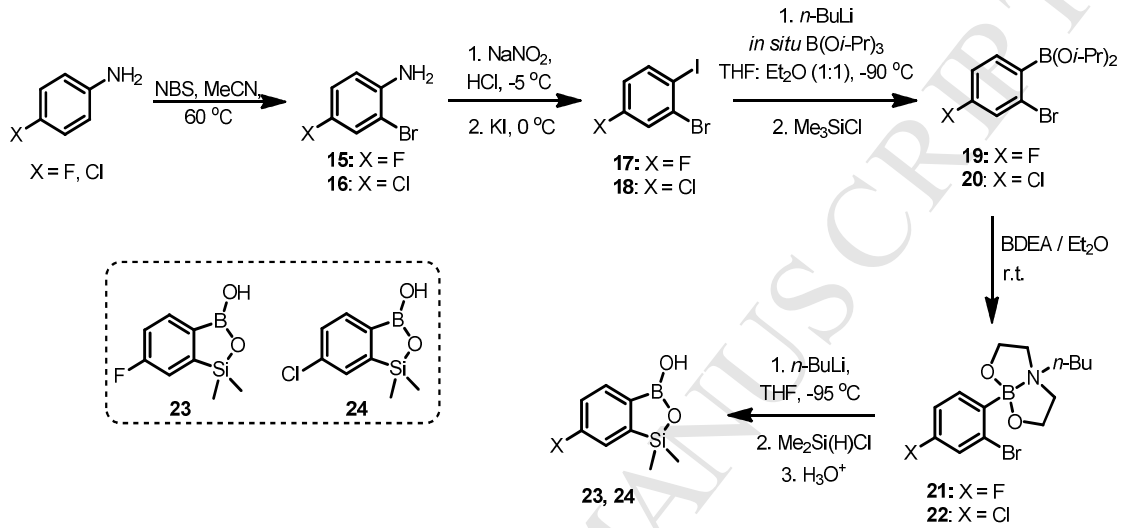

Scheme 5. Synthesis of 6-fluoro and 6-chloro substituted benzosiloxaboroles as direct analogues of tavaborole.

In the next step we have turned our attention to functionalized benzosiloxaboroles (Scheme 2, **II, III**). For these studies we have selected compounds bearing $B(OH)_2$ and CHO functional groups. We have assumed that such functionalization may be beneficial for the activity due to a stronger and specific binding to biological targets by means of hydrogen-bond interaction or direct covalent/coordination bond. With boronic group, ester formation or boron-nitrogen/oxygen coordination is expected, while in the case of formyl group hemiacetal or acetal may be formed. The geometry of the molecule may be crucial for biological activity and thus systems bearing $B(OH)_2$ or CHO groups along with some fluorine atoms at various positions have been obtained. Exceptionally 4-$B(OH)_2$ and 7-CHO derivatives were not obtained due to synthetic limitations. At this point it should be noted that the fluorine substituents play a dual role, as it allows to regulate reaction selectivity and also, as will be shown in the next paragraph, it may enhance biological activity of the system.

Synthesis of boronated derivatives **25**, **27**, and **29** (Scheme 6) was accomplished by the treatment of respective silylated dibromobenzenes **8**, **26**, **28** with an excess of *t*-BuLi which resulted in the generation of respective dilithio intermediates. Then boronation and

subsequent workup were performed as described above. In a similar way, a symmetrical species **31** composed of two siloxaborole rings fused with the central benzene ring was readily accessible from disilylated halobenzene **30**.

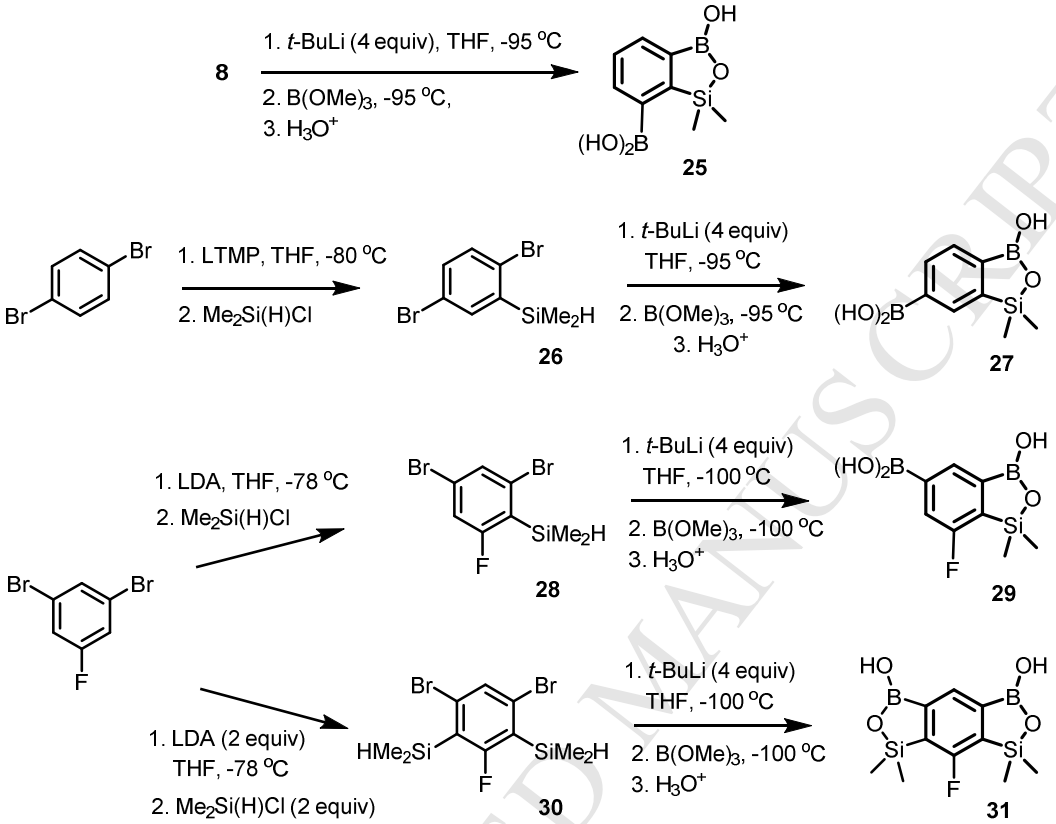

Scheme 6. Synthesis of boronic-functionalized benzosiloxaboroles.

The synthesis of formyl-functionalized compounds (**32-35**) along with some of their reduction products (**36**-**37**) were described in our recent publication (Scheme 7) [25]. Synthesis of the newly obtained compound **40** started with 1,4-dibromo-2,5-difluorobenzene and followed the general route developed for its close analogue **37**. It involves the introduction of acetal function resulting in compound **38** followed by silylation to give intermediate **39**. Final replacement of bromine atoms with boronic groups is accompanied by net reduction of acetal group with hydride bound to silicon atom (Scheme 7) [25]. A special attention should be paid to compounds **37** and **40** comprising benzoxaborole and siloxaborole rings, which may influence biological activity due to competitive or synergistic effects. It is also noticeable that the comparison between **37** and its bis(siloxaborole) analogue **31** should give additional insight into the effect of methylene/dimethylsilyl group substitution.

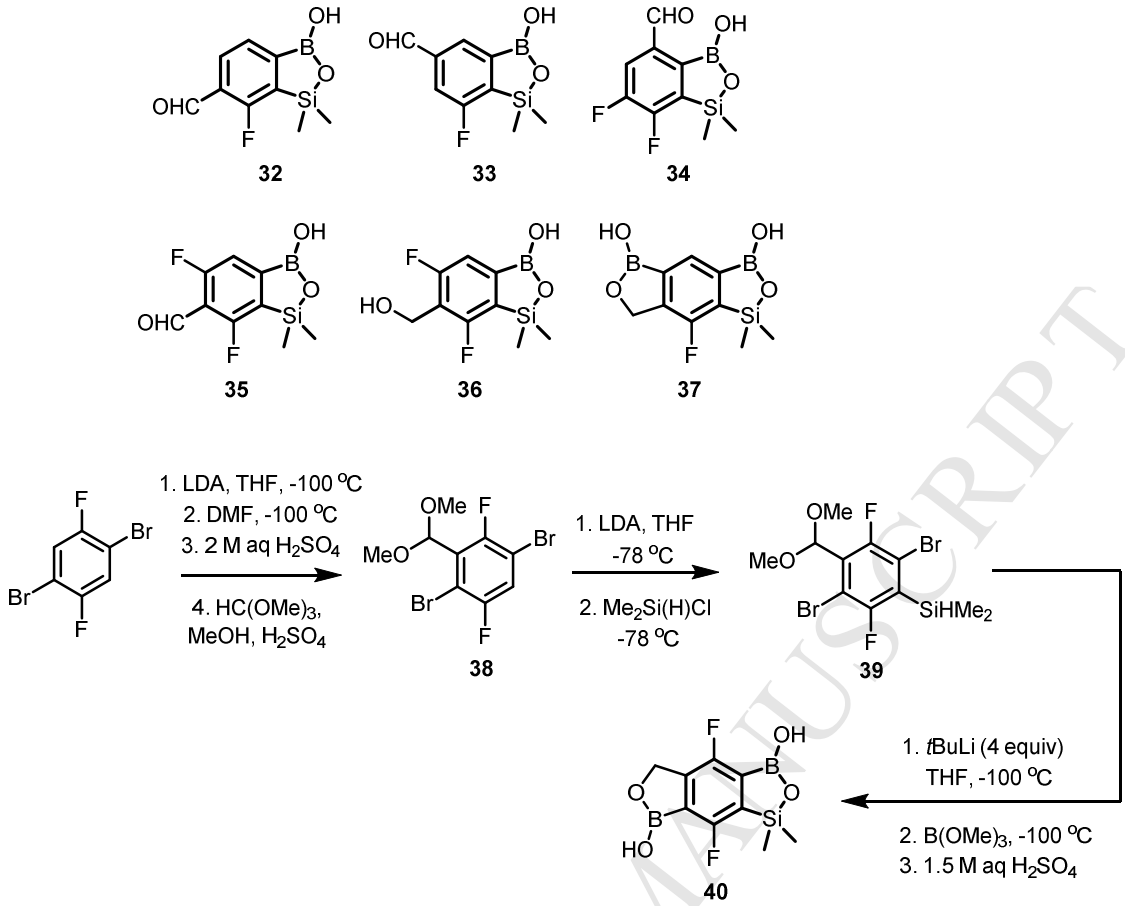

Scheme 7. Benzosiloxaboroles functionalized with CHO groups and their reduced derivatives.

All newly obtained compounds were characterized by multinuclear (^{1}H, ^{13}C, ^{11}B, ^{19}F) NMR spectroscopy. The studied benzosiloxaborole are white, air- and moisture stable solids readily soluble in polar organic solvents such as dichloromethane, acetone, MeOH and DMSO. They are also sufficiently soluble in a mixed solvent H_2O/DMSO, which is relevant to antimicrobial activity studies. Since acidity is an important parameter of a compound in view of potential medicinal chemistry applications, we have measured the pK_a values for all studied systems in water/methanol solution (1:1) by potentiometric titration with 0.1 M aq. NaOH (**Table 1**). As we have found previously, the pK_a of the parent compound **1** is 7.9 [15]. This value is lower than that determined for the benzoxaborole analogue by 0.4 pK_a units [26] reflecting the acidifying effect of the silicon centre. Acidity is strongly increased upon substitution with halogens. The introduction of formyl groups has also a positive effect on acidic properties. In the case of selected compounds possessing two boron atoms both pK_{a1} and pK_{a2} were obtained. Overall, the obtained pK_a values indicate that the most of studied compounds tend to be converted into corresponding anionic forms under standard physiological conditions (pH = 7.4), which should be beneficial for their solubility. In the

case diboron derivatives monoanionic form is expected, with hydroxyl group probably located on siloxaborole moiety.

Table 1. Acidic properties (pK_a values) of studied compounds.

	1	**2**	**3**	**4**	**10**	**11**	**12**	**13**	**14**	**23**	**24**	**25**
pK_a	7.9[a]	7.2[a]	6.8[a]	4.7[a]	6.1	6.0	6.5	6.5	6.6	7.3	7.3	7.4

	27	**29**	**31**	**32**	**33**	**34**	**35**	**36**	**37**	**40**
pK_a	7.7	6.6 10.2[b]	5.9 8.6[b]	5.4	5.6	5.2	4.9	5.8	6.3 8.6[b]	4.7 7.8[b]

[a] ref. [15]; [b] pK_{a2}

Antifungal activity

We have investigated the antifungal activity of 19 benzosiloxaboroles **1**, **10-14**, **23-25, 27**, **29, 31-38, 40** against 6 yeast strains. For comparison, we also included the data obtained for **2-4** [15]. Five species from the *Candida* genus belong to the opportunistic fungi and cause significant morbidity in people with decreased immunity. The highest mortality rate applies to patients in intensive care units, where *Candida albicans* is the fourth leading cause of nosocomial bloodstream infections [27]. Antifungal activity was determined according to Clinical and Laboratory Standards Institute (CLSI) [28,29] and European Committee on Antimicrobial Susceptibility Testing (EUCAST) [30] recommendations by disk-diffusion method and by evaluation of the MIC values. Fluconazole was used as a reference compound as it is the most commonly used antifungal compound in the case of suspected yeast infections. However, among the *Candida* genus, *Candida krusei* is intrinsically resistant to fluconazole (FL) [31,32]. The antifungal activity of the most active compounds is presented in the **Table 2** whereas complete set of data is given in the Supporting Information (**Table S1**). Halogen-substituted benzosiloxaboroles from the group **I** (**1-24**) demonstrated the highest antifungal activity (MIC 1.56-6.25 mg/L) against *Saccharomyces cerevisiae* ATCC 9763, *Candida tropicalis* IBA 171 and *Candida guilliermondii* IBA 155. The presence of chlorine at the 6-position of benzosiloxaboroles in **11** and **24** resulted in selectively higher activity of these agents against *C. albicans* ATCC 90028 (MIC 12.5 mg/L). Comparable activity in relation to fluconazole was observed for **3** and **4** against *C. tropicalis* as well as for **10** against *C. guillermondii*. Moreover, compound **23**, the structural analogue of tavaborole, demonstrated the highest activity against *S. cerevisiae* and promising activity against *Candida*

krusei and *C. tropicalis*. We have also tried to find any dependence between the acidity and activity of obtained compounds. However, the correlation is not monotonic as the highest antifungal activity was found for dihalogenated compounds **3**, **10**, **11** having the pK_a of ca. 6-7, i.e., in the middle of the pK_a range of ca. 4-8.5 found for all characterized derivatives. Introduction of additional electron-withdrawing formyl groups resulted in increased acidity (for derivatives **32-35**, pK_a = 4.9-5.6). However, the antifungal activity decreased significantly which indicates that specific structural effects can be very important. It is also plausible that an anionic form is much less effective in penetration through cell membrane due to higher hydrophilicity although it is preferentially bound in the cell interior, e.g., in an enzyme pocket. Thus, the possibility for equilibration between the neutral and anionic form under physiological conditions would be a key factor responsible for high antimicrobial activity.

Table 2. The MIC values of selected benzosiloxaboroles against yeasts.

Agent tested	MIC [mg/L]					
	C. albicans ATCC 90028	*C. parapsilosis* ATCC 22019	*C. tropicalis* IBA 171	*C. guilliermondii* IBA 155	*C. krusei* ATCC 6258	*S. cerevisiae* ATCC 9763
1	100	25	25	25	25	**3.125**
2[a]	50	100	50	**12.5**	50	**6.25**
3[a]	50	100	**0.78**	**6.25**	50	**3.125**
4[a]	200	50	**1.56**	50	200	25
10	100	**12.5**	**6.25**	**3.125**	100	**12.5**
11	**12.5**	**12.5**	**3.125**	25	**12.5**	**6.25**
23	25	25	**12.5**	25	**12.5**	**1.563**
24	**12.5**	25	**6.25**	25	25	**6.25**
FL[b]	**1**	**2**	**0.38**	**0.75**	64[c]	16[d]

The highest activity indicated by the low MIC values (0.78–12.5 mg/L) is shown in bold.

[a]The MIC values of compounds **2-4** against standard strains were previously described [15].

[b]used as a reference antifungal agent.

[c]The ellipse was visible at the MIC value 64 mg/L with macro-colonies up to ≥ 256 mg/L. The MIC value of fluconazole (≥ 256 mg/L) against *C. krusei* was given in accordance with the recommendations for Etest method [33,34].

[c]The ellipse was visible pointing the MIC value 64 mg/L, however, with macro-colonies up to concentration ≥256 mg/L. In accordance with the recommendations for Etest method, the MIC value of FL against *C. krusei* can be also interpreted as ≥256 mg/L [31,32]. *C. krusei* is intrinsically resistant to fluconazole.

[d]The ellipse was visible pointing the MIC value 16 mg/L, with colonies up to concentration ≥256 mg/L. There are no recommendations for Etest method interpretation of the MIC value of FL against *S. cerevisiae*. The obtained MIC 16 mg/L is in line with the published results [32].

Direct antibacterial activity

Inspired by reported high activity of benzoxaborole derivative- epetraborole (GSK2251052), [35-37] we have investigated the activity of benzosiloxaboroles against group of 5 Gram-positive and 10 Gram-negative strains. All data are deposited in the Supporting Information, **Tables S2-S3** and compared with those found for nitrofurantoin in accordance with EUCAST and CLSI recommendations [38,39]. All tested compounds showed a higher activity against *Staphylococcus* sp. than *Enterococcus* sp. strains (MICs 6.25-200 mg/L and 25->400 mg/L, respectively). The highest activity was observed for compound **11** and **40**, with the MICs of 6.25-25 mg/L. Moreover, Gram-positive cocci are more susceptible to chloro-substituted compounds than to their fluoro counterparts. It is also worth to pay attention to diboronic compounds **37** and **40**, for which low MICs (3.12-6.25 mg/L) for *S. aureus* and *S. epidermidis* were obtained. These values are comparable to those reported for nitrofurantoin and epetraborole [35,40]. Finally, it is noticeable that the 6-CF_3-substituted benzosiloxaborole **14** showed the highest bactericidal activity (MBC) in the range of 50-100 mg/L.

14 of 22 tested benzosiloxaboroles displayed only weak activity against Gram-negative bacilli (Table S3). The highest activity was found for **40** against *Stenotrophomonas maltophilia* ATCC 13637 and *Burkholderia cepacia* ATCC 25416 (MICs 50 mg/L). It should be stressed that MDR efflux pumps, especially those from the RND family, play a significant role in the resistance of Gram-negative bacteria to antibiotics and chemotherapeutics [41]. Therefore we undertaken the study on the influence of the efflux pump inhibitor PAβN [42,43] on the activity of our compounds. It is known that PAβN potently inhibits the efflux systems from the Mex family in *P. aeruginosa* (especially MexAB-OprM) [44,45] as well as it inhibits the AcrAB-TolC efflux system, described in the strains of the *Enterobacteriaceae* family species, e.g., *E. coli* [43], *K. pneumoniae* [46], *Proteus mirabilis* [47], *Enterobacter aerogenes* [48], and *Salmonella enterica* serovar Typhimurium [49]. We found that MIC

values for all benzosiloxaboroles significantly (at least 4-fold) decreased in the presence of PAβN for the majority of the standard strains (**Table 3**). Large decrease (from 32-fold to 64-fold) in the MIC values in the presence of PAβN was noticed in the case of chloro-substituted derivatives **11** (for 6 strains) and **24** (for 4 strains). The highest increase in bacterial susceptibility to benzosiloxaboroles in the presence of PAβN was observed also in the case **11** and **24** as MIC values decreased from 400 mg/L to 6.25 mg/L for *E. coli* and from 100–200 mg/L to 6.25 mg/L for *S. maltophilia*. Obtained results indicate that benzosiloxaboroles are effectively extruded through bacterial walls by MDR efflux pumps, and thus further studies are necessary to develop more effective systems.

β-Lactamase inhibitory activity

The β-lactamase inhibitory activity of boronic acids has been known since the late 1970's [50,51]. According to EUCAST recommendation, phenylboronic acid (PBA) is commonly used in phenotypic detection methods of KPC-producing strains among Gram-negative rods [52]. PBA inhibits also AmpC cephalosporinases [53]. A report on the ability of phenoxybenzoxaboroles to inhibit AmpC enzyme has been published [54]. Furthermore, in August 2017 U.S. FDA approved *Vabomere* containing vaborbactam in a combination with β-lactam antibiotic (meropenem) for treatment of complicated urinary tract infections (cUTIs) and acute pyelonephritis (AP), caused by carbapenem-resistant Gram-negative bacteria from *Enterobacteriaceae* family (CRE) [55,56]. Vaborbactam is based on a cyclic boronic acid pharmacophore and shows activity against Ambler classes A and C enzymes [55, 57-59].

Taking this into account, we have investigated the β-lactamase inhibitory activity of all 22 presented organoboron compounds using strains expressing the various classes of β-lactamases. In the first stage, we looked for compounds, which possess the significant β-lactamase (KPC, AmpC and ESBL) inhibitory activity at high concentrations. The screening was performed by three combination disc tests (CDTs) and PBA was used as the reference inhibitor of KPC [52] and AmpC enzymes [53]. The results are presented in **Table 3**. Interestingly for 5 out of 22 tested compounds very promising BLI activity was observed at the concentration of 0.3 mg per disc. It should be noted here that these agents (compounds **4**, **10**, **27**, **37**, **40**) are essentially inactive (MICs > 400 mg/L) against the studied Gram-negative strains when used alone (for details see **Table S3** in the Supporting Information). Compound **27** bearing the 6-$B(OH)_2$ group exhibited the highest activity. This agent inhibited the activity of KPC-2 carbapenemase as well as cephalosporinases (chromosomally encoded AmpC and plasmid encoded CMY-2). In the CDT tests, compound **27** significantly altered the diameter

of bacterial growth inhibition zone of KPC- and AmpC-producing strains around the disc with β-lactams, whereas no activity against ESBL-positive *K. pneumoniae* was detected. The BLI activity was also observed at the lower concentration 16 mg/L, however, only in the case of **27** (**Table 4** and Supporting Information, **Table S4** and **S5**). It is worth noting that vaborbactam, a new BLI at the concentration of 8 mg/L, was approved in combination with meropenem for clinical use for treatment of infections caused by CRE [55,60]. In the presence of **27** at least a four-fold decrease in the MIC values of ceftazidime and meropenem were observed for AmpC-positive and KPC-positive strains, respectively. However, our studies have shown that **27** inhibits more significantly the growth of strains producing KPC-3 rather than KPC-2 enzymes. The relationship between structure and activity was observed very clearly in the case of boronated derivatives as structural analogues of **27** with the $B(OH)_2$ group at the 5 (**25**) or 7 (**29**) positions, were not active. Moreover, in the CDT tests the BLI activity against CMY-2-producing strain was observed for derivatives **4, 10**, **37** and **40** (**Table 3**) at the concentration of 16 mg/L (Supporting Information, **Table S4** and **S5**). SAR analysis indicates that the substitution pattern plays a major role in the inhibitory activity. Unlike compounds **4** and **10** bearing two fluorine atoms at positions 6 and 7, the monofluorinated derivatives **2** and **23** as well as 5,6-difluorosubstituted derivative **3** were inactive. Also, introduction of chlorine atoms did not result in any significant activity. Finally, the AmpC inhibitory activity of compounds **37** and **40** probably results from their unique structure created through a fusion of oxaborole and siloxaborole heterocycles with a central benzene ring. Remarkably, the most promising compounds (**10**, **27**, **37**) are not cytotoxic toward human lung fibroblasts (MRC-5) in a concentration range of 1-16 µg/ml. For compounds **10** and **37**, the cell viability was decreased to 74.0±7.3% and 54.3±3.6%, respectively at the higher concentration (32 µg/ml) indicating their weak cytotoxicity (Supporting Information, Table S6).

Table 3. β-Lactamase inhibitory activity of selected benzosiloxaboroles.

Disc with antibiotic +/- studied agent[a]	Diameter of inhibition zone (mm)[b]			
	K. pneumoniae ATCC BAA 1705 KPC(+)	*P. aeruginosa* MUW 700 AmpC(+)	*E. coli* 77 CMY-2(+)	*K. pneumoniae* ATCC 700603 ESBL(+)
	MEM-10[b]	CAZ-30[b]	CAZ-30[b]	CAZ-30/CTX-30[b]
without agent	12	11	13	13/19

PBA	**22**	**22**	**24**	14/19
4	13	11	**22**	13/19
10	14	14	**22**	13/19
27	**18**	**18**	**22**	13/19
37	12	**16**	**20**	13/19
40	12	11	**20**	13/19

MEM-10: A disc with meropenem 10 μg per disc. CAZ-30: A disc with ceftazidime 30 μg per disc. CTX-30: A disc with cefotaxime 30 μg per disc. The diameter of all used antibiotic discs was 6 mm. The amount of reference compound PBA and other agents added onto the antibiotic discs was 0.3 mg per disc.

[a]The addition of compounds **1-3**, **11-14, 23-25**, **29**, **31-36** onto antibiotic discs did not significantly alter the diameter of the bacterial growth inhibition zones in comparison to the results obtained with the antibiotic discs alone.

[b]A significant difference in the inhibition zones around the antibiotic disc with an agent versus the same antibiotic disc without agent is presented in boldface. In the case of meropenem (MEM) a significant difference is at least 4 mm, while for ceftazidime (CAZ) and cefotaxime (CTX) it is at least 5 mm [52,53].

Table 4. The MICs for β-lactam antibiotics alone and in combination with **27** against standard and clinical strains of Gram-negative rods producing various classes of β-lactamases (the results for other agents are given in **Tables S4-S5** in the Supporting Information).

Strain	β-lactamase		MICs (mg/L) of antibiotic in the absence or in the presence of additional agent[a]					
		Ambler class [65]	CAZ	CAZ + PBA	CAZ **+27**	MEM	MEM +PBA	MEM **+27**
K. pneumoniae ATCC BAA-1705	KPC-2	A-CARB	64	32	64	64	**16**	32
K. pneumoniae 75	KPC-2	A-CARB	>64	**16**	64	32	16	16
E. coli 76	KPC-2	A-CARB	>64	>64	>64	>64	**32**	>64
K. pneumoniae 81[b]	KPC-3	A-CARB	64	**16**	64	16	**2**	**4**
E. coli 82 TR(pl 81)[c]	KPC-3	A-CARB	32	**8**	32	2	**0.25**	**0.25**
K. pneumoniae 83[b]	KPC-3	A-CARB	>64	**16**	64	32	**8**	**8**

	CTX-M-3	A-ESBL						
P. aeruginosa 698	VIM	B-MBL	64	64	64	16	16	16
A. baumannii 181[d]	CHDL	D-CARB	>64	>64	>64	>64	>64	>64
P. aeruginosa 700	AmpC	C	>64	**8**	**32**	0.5	0.25	0.25
E. coli 77[b]	CMY-2	C-pAmpC	32	**8**	**8**	<0.125	nd	nd
K. pneumoniae 78[e]	CMY-2	C-pAmpC	>64	**32**	64	<0.125	nd	nd
K. pneumoniae ATCC 700603	SHV-12	A-ESBL	64	64	64	<0.125	nd	nd
E. coli 557	CTX-M-2	A-ESBL	16	16	16	<0.125	nd	nd
P. aeruginosa 852	OXA-15	D-ESBL	>64	>64	>64	32	16	32

CAZ: ceftazidime. CAZ+PBA: ceftazidime with phenylboronic acid. CAZ+**27**: ceftazidime with new agent no **27**. MEM: meropenem. MEM+PBA: meropenem with phenylboronic acid. MEM+**27**: meropenem with new agent no **27**. A-CARB: class A carbapenemases. A-ESBL: class A extended-spectrum β-lactamases. B-MBL: class B metalo-β-lactamases. D-CARB: class D carbapenemases. C: class C cephalosporinases. C-pAmpC: class C plasmid-acquired AmpC cephalosporinases. D-ESBL: class D extended-spectrum β-lactamases. nd: not determined.

Significant decrease (at least 4-fold) of MIC values of β-lactam antibiotic in the presence of a tested compound are presented in boldface.

[a]All new agents and the reference compound PBA were used at the concentration of 16 mg/L.

[b]In addition, these strains produce the narrow spectrum β-lactamase TEM-1-like.

[c]The transformant of *E. coli* DH5α with plasmid from clinical strain of *K. pneumoniae* 81.

[d]This strain produces two enzymes from CHDL family: OXA-24-like and OXA-51-like.

[e]In addition, this strain produces the narrow spectrum β-lactamases TEM-1-like and OXA-1.

Docking and molecular dynamics with KPC-2 enzyme

In order to get deeper understanding of the β-lactamase inhibition mechanism we have performed the docking simulations complemented by the molecular dynamic studies on the group of the most active benzosiloxaboroles (**10**, **27**, **37**) with the KPC enzyme. To date, at least 39 variants of KPC carbapenemases have been reported [61] although KPC-2 appears to be the most widespread in the world among various types of bacteria in the *Enterobacteriaceae* family [62,63]. The RCSB Protein Data Base (PDB) contains the crystal structure of 3-nitrophenyl boronic acid (3-NPBA) bound to the KPC-2 enzyme, and this

system was used as a starting point for our calculations (**Scheme 7**) [64]. In the crystal structure, 3-NPBA interacts with Ser70, Lys73, Asn132, Asn170 and Thr237 of KPC-2 enzyme mainly through hydrogen bonds. Molecular dynamics revealed two more hydrogen bonds formed with Cys69 and Ser130. Assuming that considered compounds bind to the same site as the reference one, they should form similar interactions in order to trigger the same biological effect. As the obtained pK_a values span below 7 for most of studied systems, it is expected that the anionic forms are strongly preferred over the neutral ones. Accordingly, crystallographic data show that 3-NPBA is present in its anionic form and binds to the KPC-2 enzyme through the B-O-Ser70 covalent bond. In the case of diboron systems, the monoanionic form seems to be the most abundant under biological conditions. Nevertheless, the compound may be further ionized in a binding pocket due to a local environment. For that reason, all possible ionization states were generated. Compound **10** was considered in only one ionization state (**10a**). Compounds **27** and **37** were investigated in all three possible ionization states – with additional OH group bound to the boron atom either in benzosiloxaborole (**27a** and **37a**) or benzoxaborole ring (**27b** and **37b**, respectively), or dianionic form with two hydroxyl groups bonded to both oxaborole rings (**27ab** and **37ab**, see **Scheme 8**). For comparison we have also performed docking simulations for 4-fluorobenzoxaborole (4-FBOB), (Scheme 7). It was investigated in its neutral and anionic forms (Scheme 8).

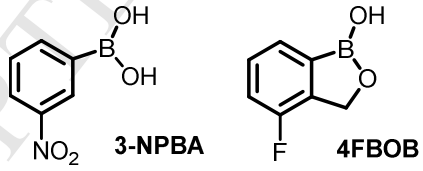

Scheme 7. Referential compounds for docking and MD simulations.

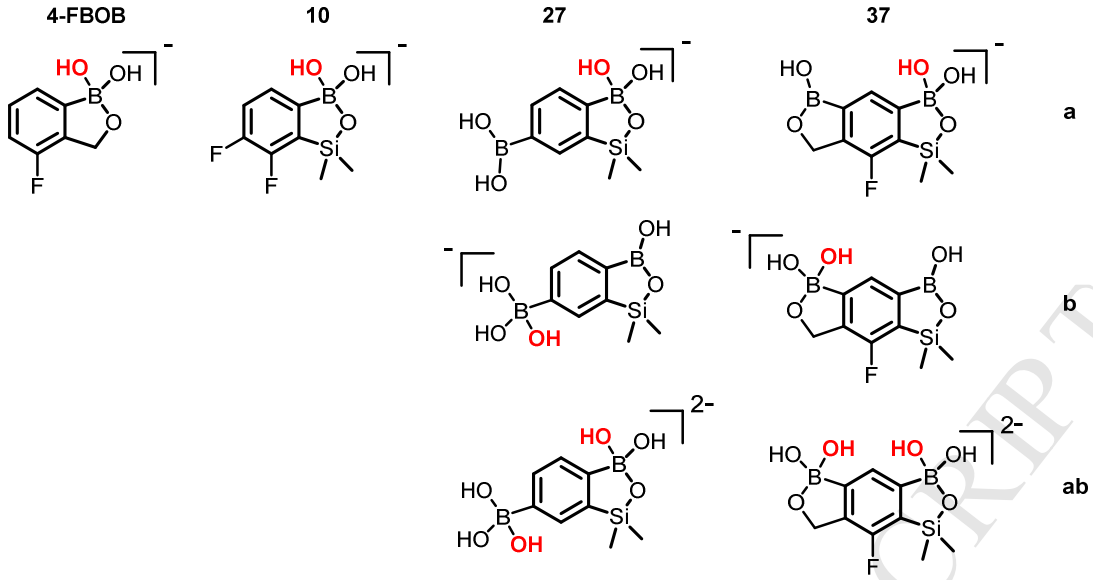

Scheme 8. Discussed anionic forms of 4FBOB, **10**, **27** and **37**.

Molecular docking results show that compounds **27** and **37** in their corresponding dianionic forms are strongly bound to the enzyme pocket. In general, all obtained modes scored between -5.5 and -5.0 kcal/mol. In the case of **27** the binding of monoanionic form **27a** with hydroxyl group attached on the oxaborole site is energetically favorable over **27b**. Conversely, the binding of **37b** is slightly more preferable than **37a**, indicating that stronger interactions are formed with ionized oxaborole ring than with siloxaborole one. This can be rationalized by the higher steric hindrance of $SiMe_2$ groups compared to the CH_2 bridge.

In the next step all anionic forms were subjected to molecular dynamics (MD) simulations. Furthermore, for each system two molecule-enzyme binding modes have been considered. The first one is based on intermolecular (non-covalent) forces such as hydrogen bonds, C-H···π interactions, etc., while the second involves the formation of the covalent B-O bond with the Ser70 moiety. The most stable modes were determined based on binding energy values in MD simulations. Their stability as well as ligand interactions were similar to those found for 3-NPBA. In every MD simulation with non-covalent binding mode, we have found that at least 3 out of 7 intermolecular interactions that are present in reference system (with Ser70, Lys73 and Thr237) have been preserved. In turn, in simulations where B-O-Ser70 covalent bond was introduced, two or three intermolecular interactions were preserved from the 3-NPBA – KPC-2 reference system (**Figure 1**). The covalent bond with Ser70 locates all compounds in the active site in such a manner that their aromatic rings are similarly oriented during the MD simulations. This indicates that studied compounds are well fitted to the active site shape.

Analysis of all forms for each compound revealed that the most stable, hence the most probable, are **10a**, **27ab**, **37a**, presenting similar interaction energies with KPC-2. For non-covalently bonded systems mean net interaction energies during the simulations are in range from –57.48 to –105.45 kcal/mol while for covalently bonded systems they are in range from –107.69 to –124.34 kcal/mol (**Table 5**). Our results indicate that in cell-free systems compound **27ab** exhibits the strongest inhibitory activity. In turn, **37a** is less effective (and comparable to 3-NPBA), whereas **10a** exhibits weaker, yet still significant binding to the KPC-2, which corresponds to results of β-lactamase inhibitor activity test (**Table 5**).

The ionization aspects of **27** seem to be particularly interesting. Since the existence of a dianionic form strongly depends on the environment, it is crucial to be determined if they can occur in this state in a bacterial cell or not. If acquiring of a dianionic form were possible, this would result in the strongest biological effect of this compound among the others yet binding to Ser70 with side **a** is still more probable than with side **b** due to its significantly lower interaction energy with KPC-2. If ionization is possible only on one side of the compound the interaction with KPC is weaker and remains on the same level as for **10a** regardless of which boron atom is directed to the interior of a KPC-2 pocket. These results should also be applicable to KPC-3 containing systems. The sequence alignment of KPC-2 and -3 revealed that the only difference between these proteins in a region close to binding pocket is a single amino acid substitution. Instead of His274 residue, the KPC-3 contains Tyr272 structurally located in the same position. However, this particular amino acid does not take part in ligand binding directly and it is separated from the binding site by Thr237 (KPC-2 numbering).

The obtained results have been compared to referential system 4-FBOB. We observed that its docking scores are significantly lower than in benzosiloxaboroles, ranging from -4.2 to -3.9 kcal/mol. Similarly to all other investigated compounds, the ionized form is energetically favorable over the neutral one. In MD simulations, the interactions with Ser70, Thr237 are preserved, however the interaction with Lys73 is replaced with Lys234 residue. This behavior is a consequence of lack of two Si-bound Me groups in 4-FBOB, which limits its mobility in the binding site. 4-FBOB in its non-covalently bounded form is displaced by about 1 Å as compared to the location of **10a**. After formation of the covalent bond it rearranges to the same position as in the other compounds. Summing up, the performed calculations show that the benzosiloxaboroles interact less effectively with KPC-2 in their non-covalently bounded forms than benzoxaboroles. Conversely, it seems that the covalent binding of benzosiloxaboroles is more advantageous than for benzoxaboroles represented by 4-FBOB.

Table 5. Interactions with KPC-2 for compounds 3-NPBA, 4-FBOB, **10a**, **27ab** and **37a**.

Compound	Net interaction energy (mean ± SEM kcal/mol)		Amino acids contacts
	Non-covalently bound	Covalently bound	
3-NPBA	- 97.28 ± 0.11	-116.95 ± 0.12	Cys69, Ser70, Lys73, Ser130, Asn132, Asn170, Thr237
4-FBOB	-98.36 ± 0.23	-95.70 ± 0.07	Ser70, Lys73/Lys234, Ser130, Asn132, Asn170, Thr237
10a	- 57.48 ± 0.14	-107.69 ± 0.07	Ser70, Lys73, Asn132, Asn170, Thr237
27ab	- 75.11 ± 0.12	-124.34 ± 0.34	Cys69, Ser70, Lys73, Ser130, Asn132, Asn170, Arg220, Thr237
37a	- 105.45 ± 0.11	-113.37 ± 0.07	Ser70, Lys73, Asn170, Thr237

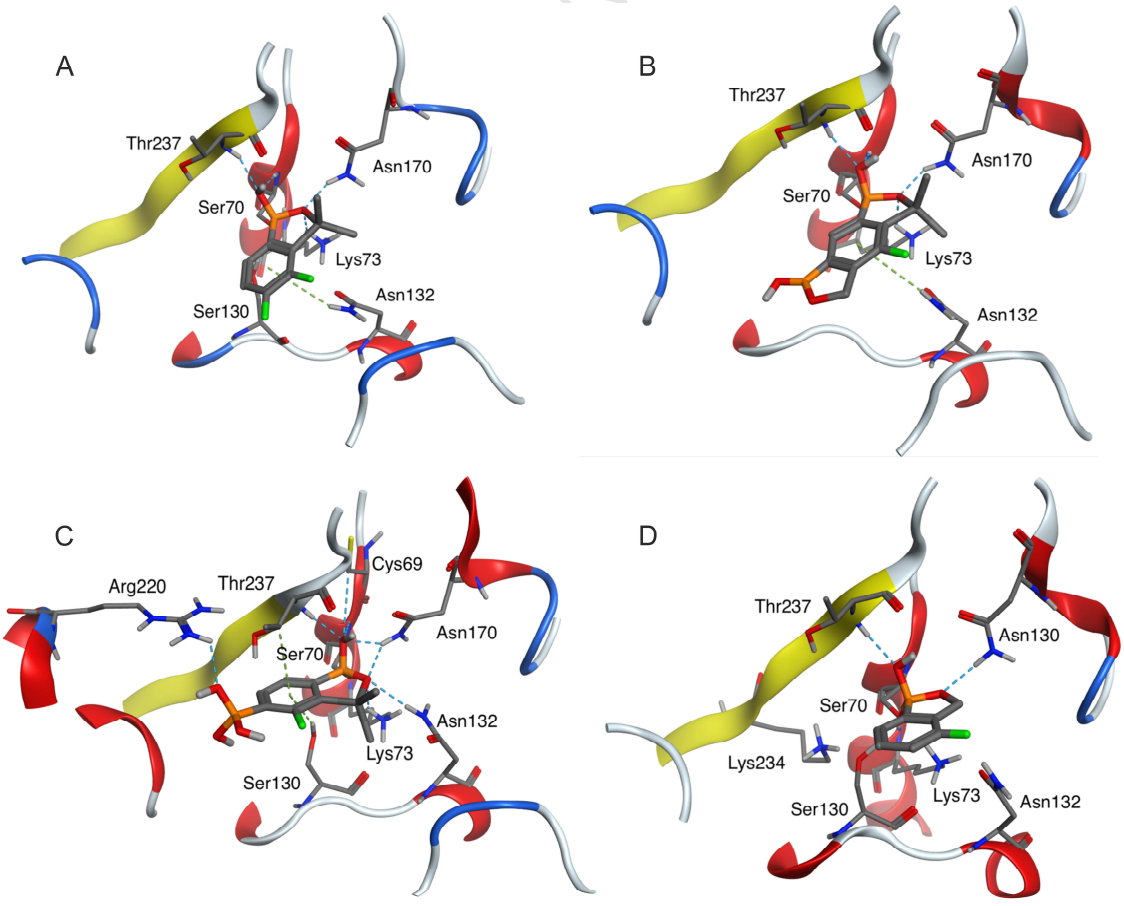

Figure 1. KPC-2 (PDB ID: 3RXX [62]) contacts formed with compounds **10a** (A), **37a** (B), **27ab** (C) and 4-FBOB (D). Visible amino acids form interactions with compounds. Blue and green dashed lines depict hydrogen bonding and C-H···π interactions, respectively.

Conclusions

In conclusion, a series of benzosiloxaboroles with varying substitution patterns were obtained and their biological properties were comprehensively studied in order to elucidate the structural factors that affect their bioactivities. Most of compounds were prepared from simple starting materials based on two general protocols elaborating introduction of silicon-containing group in the first step followed by the Br/Li exchange and boronation, or the reversed one. In selected cases (especially, for compounds **23** and **24**) multistep reaction sequences were developed. We would like to stress that the synthesis of benzosiloxaboroles is relatively simple as compared to many biologically active systems currently used in medicine. This indicates that they can be easily accessed on a significant scale that can allow their further use toward desired application.

The most significant result of this work is demonstration of the KPC/AmpC enzyme inhibitory activity by some benzosiloxaboroles (compounds **4, 10**, **27, 37** and **40**). The highest activity was observed for 6-$B(OH)_2$ substituted derivative **27**. Biological activity of selected compounds has been confirmed with molecular modelling methods. Docking results with KPC-2 enzyme showed the strongest binding with compounds **27** and **37**. Importantly, they also exhibit low cytotoxity as indicated from the tests performed for human lung fibroblast. At this point it should be stressed, that only one organoboron compound, namely vaborbactam, was approved for treatment as a novel β-lactamase inhibitor with KPC inhibitory activity, so far. Thus our results may initiate new progress in this area.

Moreover, obtained series of benzosiloxaboroles showed direct antifungal activity, especially against *C. tropicalis*, *C. guilliermondii* and *S. cerevisiae*. The presence of chlorine at the 6-position of benzosiloxaboroles in compounds **11** and **24** resulted in selectively higher activity of these agents against *C. albicans*. It is interesting that **11** showed also the highest activity against Gram-positive cocci from *Staphylococcus* and *Enterococcus* genera (MIC values 6.25 mg/L and 25 mg/L, respectively). The clinical strains of *S. aureus* MRSA and *E. faecalis* VRE are still a severe health public problem. Regarding the weak activity against Gram-negative rods, the MIC values for a group of 22 studied benzosiloxaboroles in the presence of PAβN were significantly (a minimum 4-fold) reduced against majority of the

studied strains. Presumably, a limited activity (MIC 100->400 mg/L) of analyzed compounds resulted from the presence of specific Gram-negative rods efflux pumps.

To summarize, our study highlights a new group of organoboron heterocycles as a source of potential KPC inhibitors as well as direct antifungal agents. Further work in the field is currently in progress in our group and the results will be given in due course. The search for organoboron compounds that inhibit β-lactamases, particularly carbapenemases, is one of the latest ways to look for new therapeutic options. The rapid progress in this field is highly demanded as the mortality of patients infected with KPC-producing strains reaches 70%, constituting one of the major worldwide health threats [65,66].

Experimental Section

Synthesis of benzosiloxaboroles.

Solvents used for reactions were dried by heating to reflux with sodium/benzophenone and distilled under argon. *n*-BuLi (10 M in hexane), *t*-BuLi (1.7 M in pentane), trialkyl borates $B(OR)_3$, $Me_2Si(H)Cl$ and starting haloarenes were used as received without further purification. Detailed procedures for the synthesis of benzosiloxaborole precursors are given in the Supporting Information. Syntheses of benzosiloxaboroles **1**-4 [15] and **32**-**37** [25] were reported by us recently. In the ^{13}C NMR spectra the resonances of boron-bound carbon atoms were not observed in most cases as a result of broadening by a quadrupolar boron nucleus. ^{1}H and ^{13}C NMR chemical shifts are given relative to TMS using residual solvent resonances. ^{11}B and ^{19}F NMR chemical shifts are given relative to $BF_3{\cdot}Et_2O$ and $CFCl_3$, respectively. The purity of all new compounds (> 95%) was established by elemental analysis and HRMS.

6,7-Difluoro-1,3-dihydro-3-hydroxy-1,1-dimethyl-1,2,3-benzosiloxaborole (**10**): A solution of **5** (5.67 g, 0.023 mol) in Et_2O (10 mL) was added dropwise to a solution of *t*BuLi (1.7 M in pentane, 28.2 mL, 0.048 mol) in Et_2O (100 mL) and cooled to –95 °C. The solution was stirred for 30 min, warmed to –85 °C and then again cooled to –100 °C followed by the addition of $B(OEt)_3$ (3.9 mL, 0.023 mol). The obtained white slurry was warmed to –30 °C, quenched with 1.5 M aq. H_2SO_4 to reach the pH = 2-3 and stirred at room temperature until evolution of H_2 ceased. The aqueous phase was separated followed by the extraction with Et_2O (2 × 20 mL). The extracts were added to the organic phase, which was concentrated under reduced pressure. Water (5 mL) acidified with a few drops of conc. aqueous HCl was added and the white solid precipitated during the evaporation. It was filtered, and

recrystallized from hexane. Drying in vacuo afforded **10** as white powder, m.p. 81–82 °C. Yield 3.69 g (75%). ^{1}H NMR (400 MHz, $CDCl_3$): δ 7.53 (dd, J = 7.8, 3.8 Hz, 1H, Ar), 7.25 (ddd, J = 10.8, 7.8, 7.4 Hz, 1H, Ar), 5.20 (br, 1H, B(OH)), 0.51 (s, 6H, $SiMe_2$) ppm. ^{13}C{^{1}H} NMR (100.6 MHz, $CDCl_3$): δ 152.09 (dd, J = 254.5, 15.3 Hz), 151.51 (dd, J = 247.0, 11.6 Hz), 137.96 (d, J = 26.7 Hz), 128.84 (dd, J = 6.1, 3.5 Hz), 120.00 (d, J = 17.9 Hz), –0.76 ppm. ^{19}F NMR (282.44 MHz, $CDCl_3$): δ –129.53 (dd, J = 24.0, 7.3 Hz), –135.13 (ddd, J = 24.0, 10.8, 3.7 Hz) ppm. ^{11}B NMR (96.32 MHz, $CDCl_3$): δ 29.7 ppm. HRMS (EI): calcd. for $C_8H_9BF_2O_2Si$ $[M]^+$ 214.0433; found 214.0431. Anal. Calcd for $C_8H_9BF_2O_2Si$: C, 44.89; H, 4.24. Found: C, 44.71; H, 3.97.

6,7-Dichloro-1,3-dihydro-3-hydroxy-1,1-dimethyl-1,2,3-benzosiloxaborole (**11**). This compound was obtained from **6** (0.01 mol) using the procedure described for **10.** The product was obtained as a white powder, m.p. 107-109 °C. Yield 1.74 g (68%). ^{1}H NMR (400 MHz, $CDCl_3$): δ 7.62 (dd, J = 7.7, 2.5 Hz, 1H, Ar), 7.53 (d, J = 7.7 Hz, 1H, Ar), 0.53 (s, 6H, $SiMe_2$) ppm. ^{13}C{^{1}H} NMR (101 MHz, $CDCl_3$): δ 151.80, 135.33, 135.16, 132.54, 130.79, –1.59 ppm. HRMS (EI): calcd. for $C_8H_9BCl_2O_2Si$ $[M]^+$ 245.9842; found 245.9844. Anal. Calcd for $C_8H_9BCl_2O_2Si$: C, 38.91; H, 3.67. Found: C, 38.69; H, 3.59.

7-Chloro-1,3-dihydro-3-hydroxy-1,1-dimethyl-1,2,3-benzosiloxaborole (**12**). This compound was obtained from **7** (0.01 mol) using the procedure described for **10.** The product was obtained as a white powder, m.p. 133-134 °C. Yield 1.74 g (68%). ^{1}H NMR (300 MHz, $CDCl_3$): δ 7.67 (dd, J = 4.7, 3.4 Hz, 1H, Ar), 7.45 – 7.38 (m, 2H, Ar), 4.95 (s, 1H, B(OH)), 0.50 (s, 6H, $SiMe_2$) ppm. ^{13}C{^{1}H} NMR (100.6 MHz, $CDCl_3$): δ 149.38, 137.68, 131.76, 130.54, 129.45, –1.45 ppm. ^{11}B NMR (96.3 MHz, $CDCl_3$): δ 29.6 ppm. HRMS (EI): calcd. for $C_8H_{10}BClO_2Si$ $[M]^+$ 212.0232; found 212.0234. Anal. Calcd for $C_8H_{10}BClO_2Si$: C, 45.22; H, 4.74. Found: C, 44.76; H, 3.91.

7-Bromo-1,3-dihydro-3-hydroxy-1,1-dimethyl-1,2,3-benzosiloxaborole (**13**). This compound was obtained from **8** (0.01 mol) using the procedure described for **10.** However in this case *n*BuLi (10 M, 1.05 mL, 10.5 mmol) was used instead of *t*BuLi. The product was obtained as a white powder, m.p. 120-122 °C. Yield 1.12 g (43%). ^{1}H NMR (300 MHz, $CDCl_3$): δ 7.76 (dd, J = 7.2, 0.9 Hz, 1H, Ar), 7.58 (dd, J = 7.9, 0.9 Hz, 1H, Ar), 7.33 (dd, J = 8.0, 7.2 Hz, 1H, Ar), 6.22 (br, 1H, B(OH)), 0.54 (d, J = 0.8 Hz, 6H $SiMe_2$) ppm. ^{13}C{^{1}H} NMR (100.57 MHz, $CDCl_3$): δ 152.33, 133.62, 131.93, 130.03, 126.55, –1.64 ppm. ^{11}B NMR (96.3 MHz, $CDCl_3$): δ 29.8 ppm. HRMS (EI): calcd. for $C_8H_{10}BBrO_2Si$ $[M]^+$ 255.9726; found 255.9729. Anal. Calcd for $C_8H_{10}BBrO_2Si$: C, 37.39; H, 3.92. Found: C, 37.58; H, 3.63.

6-Trifluoromethyl-1,3-dihydro-3-hydroxy-1,1-dimethyl-1,2,3-benzosiloxaborole (**14**): This compound was obtained from **9** (0.035 mol) using the procedure described for **10**. The product was obtained as a white powder, m.p. 101-103 °C. Yield 4.90 g (71%). ^{1}H NMR (400 MHz, $CDCl_3$): δ 7.94 (dd, J = 7.7, 0.8 Hz, 1H, Ar), 7.86 (m, 1H, Ar), 7.71 (dd, J = 7.7, 0.9 Hz, 1H, Ar), 5.87 (br, 1H, B(OH)), 0.48 (s, 6H, $SiMe_2$) ppm. ^{13}C{^{1}H} NMR (101 MHz, $CDCl_3$): δ 151.00, 132.43 (q, J = 31.7 Hz, CF_3), 131.58, 126.89 (q, J = 3.8 Hz), 126.34 (q, J = 3.8 Hz), 125.66, 122.95, –0.74 ppm. ^{19}F NMR (282.44 MHz, $CDCl_3$): δ –62.74 ppm. ^{11}B NMR (96.3 MHz, $CDCl_3$): δ 30.2 ppm. HRMS (EI): calcd. for $C_9H_{10}BO_2F_3Si$ $[M]^+$ 246.0495; found 246.0497. Anal. Calcd for $C_9H_{10}BO_2F_3Si$: C, 44.93; H, 4.10. Found: C, 44.17; H, 4.12.

6-Fluoro-1,3-dihydro-3-hydroxy-1,1-dimethyl-1,2,3-benzosiloxaborole (**23**). A solution of **21** (5.16 g, 0.015 mol) in THF (15 mL) was added to the previously prepared solution of *n*BuLi (10 M solution in hexanes, 1.5 mL, 0.015 mol) in THF (30 mL) at –95 °C. After 30 min of stirring $Me_2(H)SiCl$ (1.66 mL, 0.015 mol) was slowly added. Then it was warmed gradually to –40 °C, which resulted in a white, thick slurry. It was quenched with H_2SO_4 (1.5 M) to pH = 4 and stirred at 40 ^{o}C until hydrogen evolution ceased. The water phase was separated followed by the extraction with Et_2O (2 × 20 mL). The extracts were added to the organic phase, which was concentrated under reduced pressure, to give a white residue. It was crystallized from hexane (20 mL) to give **23** as a white powder, m.p. 63-64 °C. Yield: 1.76 g (60%). ^{1}H NMR (300 MHz, $CDCl_3$): δ 7.82 (ddd, J = 8.2, 5.4, 0.6 Hz, 1H, Ar), 7.27 (ddd, J = 8.2, 2.4, 0.6 Hz, 1H, Ar), 7.14 (ddd, J = 9.7, 8.1, 2.4 Hz, 1H, Ar), 6.02 (br, 1H, OH), 0.45 (s, 6H, $SiMe_2$) ppm. ^{13}C{^{1}H} NMR (101 MHz, $CDCl_3$): δ = 165.02 (d, J = 252.6 Hz), 153.41 (d, J = 5.8 Hz), 133.62 (d, J = 7.8 Hz), 117.05 (d, J = 21.5 Hz), 116.89 (d, J = 19.0 Hz), –0.74 ppm. ^{19}F NMR (376 MHz, $CDCl_3$): δ –109.33 (ddd, J = 9.7, 8.1, 5.2 Hz) ppm. ^{11}B NMR (96 MHz, $CDCl_3$): δ 30.0 ppm. HRMS (EI): calcd. for $C_8H_{10}BO_2FSi$ $[M]^+$ 196.0527; found 196.0524. Anal. Calcd for $C_8H_{10}BO_2FSi$: C, 49.01; H, 5.14. Found: C, 48.82; H, 5.10.

6-Chloro-1,3-dihydro-3-hydroxy-1,1-dimethyl-1,2,3-benzosiloxaborole (**24**). This compound was obtained from **22** (2.38 g, 5.8 mol) using the procedure described for **23**. Yield: 0.67 g (55%), m.p. 105-108 °C ^{1}H NMR (400 MHz, $CDCl_3$): δ 7.75 (dd, J = 7.9, 0.7 Hz, 1H, Ar), 7.57 (d, J = 1.9 Hz, 1H, Ar), 7.43 (ddd, J = 7.9, 1.9, 0.5 Hz, 1H, Ar), 6.06 (s, 1H, OH), 0.45 (s, 6H, $SiMe_2$) ppm. ^{13}C{^{1}H} NMR (75 MHz, $CDCl_3$): δ 152.43, 137.76, 132.80, 130.41, 129.90, -0.68 ppm. ^{11}B NMR (96 MHz, $CDCl_3$): δ 30.0 ppm. HRMS (EI): calcd. for $C_8H_{10}BO_2SiCl$ $[M]^+$ 212.0232; found 212.0225. Anal. Calcd for $C_8H_{10}BO_2SiCl$: C, 45.22; H, 4.74. Found: C, 44.85; H, 4.39.

1,3-Dihydro-3-hydroxy-7-(dihydroxyboryl)-1,1-dimethyl-1,2,3-benzosiloxaborole (**25**). This compound was obtained from **8** (5.88 g, 0.02 mol) in a similar procedure as **10**. 4 equiv of *t*BuLi (1.7 M pentane, 47 mL, 0.08 mol) and 3 equiv of $B(OMe)_3$ (6.4 mL, 0.06 mol) were used. The product was obtained as a white powder, m.p. 340-344 °C. Yield 3.30 g (74 %). ^{1}H NMR (400 MHz, acetone-d_6 + D_2O): δ 7.97 (dd, J = 7.4, 1.2 Hz, 1H, Ar), 7.87 (dd, J = 7.3, 1.2 Hz, 1H, Ar), 7.39 (t, J = 7.4 Hz, 1H, Ar), 3.93 (br, 3H, OH), 0.34 (s, 6H) ppm. ^{13}C NMR (101 MHz, acetone-d_6 + D_2O): δ 158.16, 135.99, 132.87, 128.45, -1.15 ppm. ^{11}B NMR (96 MHz, acetone-d_6 + D_2O) δ 28.8 ppm. HRMS (EI): calcd. for $C_8H_{12}B_2O_4Si$ $[M]^+$ 222.0691; found 222.0690. Anal. Calcd for $C_8H_{12}B_2O_4Si$: C, 43.31; H, 5.45. Found: C, 43.40; H, 5.79.

1,3-Dihydro-3-hydroxy-6-(dihydroxyboryl)-1,1-dimethyl-1,2,3-benzosiloxaborole (**27**). This compound was obtained from **26** (2.95 g, 0.01 mol) using the procedure described for **25.** Yield 1.57 g (71%). m.p. 340-346 ^{o}C. ^{1}H NMR (300 MHz, acetone-d_6 + D_2O): δ 8.16 (s, 1H, Ar), 7.92 (d, J = 7.5 Hz, 1H, Ar), 7.82 (d, J = 7.5 Hz, 1H, Ar), 3.61 (br, 3H, OH), 0.36 (s-br, 6H, $SiMe_2$) ppm. ^{13}C NMR (101 MHz, acetone-d_6 + D_2O): δ 149.14, 136.33, 134.98, 130.15, –1.36 ppm. ^{11}B NMR (96 MHz, acetone-d_6 + D_2O): δ 28.8 ppm. HRMS (EI): calcd. for $C_8H_{12}B_2O_4Si$ $[M]^+$ 222.0691; found 222.0689. Anal. Calcd for $C_8H_{12}B_2O_4Si$: C, 43.31; H, 5.45. Found: C, 42.94; H, 5.80.

7-Fluoro-1,3-dihydro-3-hydroxy-5-(dihydroxyboryl)-1,1-dimethyl-1,2,3-benzosiloxaborole (**29**). A solution of **28** (3.12 g, 0.01 mol) in Et_2O (15 mL) was added dropwise to a solution of *t*-BuLi (1.7 M in pentane, 24 mL, 0.04 mol) in THF (70 mL) at –100 °C. After 30 min of stirring at –100 °C, $B(OMe)_3$ (4.4 mL, 0.04 mol) was added and the reaction mixture was warmed to –30 °C, quenched with 1.5 M aq. H_2SO_4 to reach the pH = 2-3 and stirred at room temperature until evolution of H_2 ceased. The aqueous phase was separated followed by the extraction with Et_2O (2 × 20 mL). The extracts were added to the organic phase, which was concentrated under reduced pressure. The white solid precipitated during the evaporation. It was filtered and washed several times with water. Then it was suspended in CH_2Cl_2 (10 mL) and stirred for 30 min. Then hexane (10 mL) was added and the resulting slurry was filtered. The product was washed with hexane (2 × 5 mL) and dried *in vacuo* to give **29**, m.p. 310–315 °C. Yield 2.1 g (87%). ^{1}H NMR (400 MHz, acetone-d_6): δ 8.19 (s, 1H, BOH), 8.12 (d, J = 3.0 Hz, 1H, Ph), 7.57 (d, J = 8.2 Hz, 1H, Ph), 7.43 (s, 2H, $B(OH)_2$), 0.43 (s, 6H, $SiMe_2$) ppm. ^{13}C NMR (101 MHz, acetone-d_6): δ 164.63 (d, J = 243.5 Hz), 143.8 (broad, C_B), 139.6 (broad, C_B), 136.85 (d, J = 30 Hz), 133.30 (d, J = 2.4 Hz), 121.48 (d, J = 22.2 Hz), –1.51 (s) ppm. ^{11}B NMR (96 MHz, acetone-d_6): δ 28.5 ppm. ^{19}F NMR (376 MHz, acetone-d_6): δ –107.14 (m) ppm. HRMS (EI): calcd. for $C_8H_{11}B_2O_4Si_2F$

$[M]^+$ 240.0597; found 240.0593. Anal. Calcd for $C_8H_{11}B_2O_4Si_2F$: C, 40.06; H, 4.62. Found: C, 39.98; H, 4.58.

8-Fluoro-1,3,5,7-tetrahydro-3,5-dihydroxy-1,1,7,7-tetramethylbenzo[1,2,3,7,6,5]bis(siloxaborole) (31). This compound was prepared as described for **29** starting with **30.** It was isolated as a white solid, m.p. 136–140 °C. Yield 2.2 g (74%). ^{1}H NMR (300 MHz, acetone-d_6): δ 8.20 (broad, 2H, BOH), 8.09 (d, J = 5.1 Hz, 1H, Ph), 0.46 (s, 12H, $SiMe_2$) ppm. ^{13}C NMR (101 MHz, acetone-d_6): δ 166.89 (d, J = 247.0 Hz), 148.87 (broad, C_B), 136.70 (d, J = 34.3 Hz), 130.63 (d, J = 2.8 Hz), –1.45 (s) ppm. ^{11}B NMR (96 MHz, acetone-d_6): δ 29.5 ppm. ^{19}F NMR (282 MHz, acetone-d_6) δ = –96.62 (s) ppm. HRMS (EI): calcd. for $C_{10}H_{15}B_2O_4Si_2F$ $[M]^+$ 296.0679; found 296.0675. Anal. Calcd for $C_{10}H_{15}B_2O_4Si_2F$: C, 40.58; H, 5.11. Found: C, 40.33; H, 5.25.

4,8-difluoro-3,3-dimethyl-3,7-dihydro-1H,5H-[1,2]oxaborolo[4',3':4,5]benzo[1,2-c][1,2,5]oxasilaborole-1,5-diol (**40**). A solution of **39** (4.04 g, 0.01 mol) in THF (15 mL) was added dropwise to a solution of *t*-BuLi (1.7 M in pentane, 24 mL, 0.04 mol) in THF (80 mL) and cooled to –100 °C. After 30 min of stirring at –100 °C, $B(OMe)_3$ (4.5 mL, 0.04 mol) was added and the reaction mixture was warmed to –30 °C, quenched with 1.5 M aq. H_2SO_4 to reach the pH = 2-3 and stirred at room temperature. The aqueous phase was separated followed by the extraction with Et_2O (2 × 20 mL). The extracts were added to the organic phase, which was concentrated under reduced pressure. A solid residue was washed with water, CH_2Cl_2 (2 × 5 mL), hexane (2 × 5 mL), and dried *in vacuo* to give the final product **40**, m.p. 195–198 °C. Yield 0.75 g (28%). ^{1}H NMR (400 MHz, acetone-d_6): δ 5.08 (s, 2H), 2.95 (s, 1H), 0.45 (s, 6H) ppm. ^{13}C NMR (101 MHz, acetone-d_6): δ 161.3 (d, J = 244.6 Hz), 156.0 (dd, J = 251.0, 3.0 Hz), 144.8 (dd, J = 20.7, 8.0 Hz), 136.1 (d, J = 39.6 Hz), 120.65, 67.0, –1.67 ppm. ^{19}F NMR (376 MHz, acetone-d_6): δ –104.43 (dd, J = 33.5, 9.8 Hz), –121.66 (d, J = 33.5 Hz) ppm. ^{11}B NMR (96 MHz, acetone-d_6): δ 30.5 ppm. HRMS (EI): calcd. for $C_9H_{10}B_2F_2O_4Si$ $[M]^+$ 270.0503; found 270.0492. Anal. Calcd for $C_9H_{10}B_2F_2O_4Si$: C, 40.05; H, 3.74. Found: C, 40.28; H, 3.58.

Antimicrobial activity

Bacterial and fungal strains and their growth conditions. The following standard strains to determine the direct antimicrobial activity were used in the study: (1) Gram-positive cocci: *Staphylococcus aureus* ATCC 6538P, *S. epidermidis* ATCC 12228, *Enterococcus faecalis* ATCC 29212, *E. faecium* ATCC 6057, *Bacillus subtilis* ATCC 6633; (2) Gram-negative bacteria from *Enterobacteriaceae* family: *Escherichia coli* ATCC 25922, *Klebsiella*

pneumoniae ATCC 13883, *Proteus mirabilis* ATCC 12453, *Enterobacter cloacae* DSM 6234, *Serratia marcescens* ATCC 13880; (3) Gram-negative non-fermentative rods: *Pseudomonas aeruginosa* ATCC 27853, *Acinetobacter baumannii* ATCC 19606, *Stenotrophomonas maltophilia* ATCC 13637, *Burkholderia cepacia* ATCC 25416, *Bordetella bronchiseptica* ATCC 4617; (4) yeasts: *Candida albicans* ATCC 90028, *C. parapsilosis* ATCC 22019, *C. tropicalis* IBA 171, *C. guilliermondii* IBA 155, *C. krusei* ATCC 6258 and *Saccharomyces cerevisiae* ATCC 9763.

The following strains (see **Table 4**) were used to examine β-lactamase inhibitory activity of studied agents: (1) two standard strains - *K. pneumoniae* ATCC BAA-1705 (with carbapenemase KPC-2) and *K. pneumoniae* ATCC 700603 (with extended-spectrum β-lactamase, ESBL, SHV-12); (2) eleven clinical isolates producing various classes of β-lactamases – carbapenemases KPC-2 (*E. coli* 76, *K. pneumoniae* 75) and KPC-3 (*K. pneumoniae* 81 and 83), metallo-β-lactamase from VIM family (*P. aeruginosa* 698), carbapenem-hydrolyzing class D β-lactamase (CHDL) from OXA-24 family (*A. baumannii* 181), ESBL-type enzymes CTX-M-2 (*E. coli* 557) and OXA-15 (*P. aeruginosa* 852), plasmid-acquired AmpC cephalosporinase CMY-2 (*E. coli* 77, *K. pneumoniae* 78), and with overexpression of chromosomally encoded cephalosporinase AmpC (*P. aeruginosa* MUW 700); (3) the transformant of *E. coli* DH5α with plasmid from clinical strain of *K. pneumoniae* 81 carrying the gene $bla_{\text{KPC-3}}$. All strains were stored at −80 °C. Prior to testing, each bacterial strain was subcultured twice on tryptic soy agar TSA (bioMérieux) medium and yeast strains on Sabouraud dextrose agar (bioMérieux) for 24–48 h at 30 °C to ensure viability.

Determination of antimicrobial activity. Direct antimicrobial activity against yeast, Gram-positive and Gram-negative bacterial strains was examined by the disc-diffusion test and the MIC determination assays according to the EUCAST [30,67] and CLSI [28,29,66] recommendations. Additionally, in the study of antimicrobial activity of new benzosiloxaboroles two following reference agents were used: fluconazole (in the case of fungi) and nitrofurantoin (for bacteria). The MIC value of fluconazole was tested by Etest method [31,32]. Determination of MIC/MBC values of nitrofurantoin was done using the CLSI methods [68,69], however, its concentration range was compatible with Etest. The solutions of all tested compounds were prepared in DMSO (Sigma). The disc-diffusion test was determined on Mueller-Hinton II agar medium (MHA) (Becton Dickinson) for bacteria and on MHA supplemented with 2% glucose and 0.5 mg/L methylene blue dye (Sigma) (MHA+GMB medium) for yeasts. The MIC determination was performed in Mueller-Hinton

II broth medium (MHB) (Becton Dickinson) for bacteria and in RPMI 1640 broth medium (Sigma) with 2% glucose (Sigma) for yeasts. Results of antimicrobial activity were evaluated after incubation at 35 ^{o}C for 18 h (bacteria) and 24 h (yeasts). Determination of bactericidal (MBC) activity was performed according to the CLSI recommendations [69].

Determination of the MICs of agents in the presence of PAβN. To determine the ability of the strains to remove benzosiloxaboroles by MDR efflux pumps, the MIC values of studied agents, with or without the pump inhibitor, PAβN (50 mg/L) (Sigma) were evaluated [41]. The MIC determination was performed in MHB with 1 mM $MgSO_4$ (Sigma), using 2-fold serial dilutions, according to the CLSI guidelines [68] in order to compare these two assays. The presence of 1 mM $MgSO_4$ stabilizes the outer membrane [70]. At least a 4-fold decrease in the MIC value after the addition of PAβN was considered significant [40,41].

Study of BLI activity of tested agents

The ability of new studied agents to serve as BLIs was examined into two steps, initially by using combination disc tests (CDTs) for screening all compounds and then by microdilution test for selected agents.

Combination disc tests for detection of BLI activity. The three following CDTs were performed on Müller-Hinton agar (MHA) plates (Becton Dickinson) according to the general EUCAST recommendations [52] and methodology described by Yagi et al. [53]:

(1) CDT-KPC is the EUCAST phenotypic test using discs with meropenem (MEM-10) (Becton Dickinson) alone and discs with this β-lactam supplemented with PBA (Sigma) at the concentration of 0.3 mg per disc. Additionally, in this research the discs with meropenem supplemented with one of the studied compounds (at the concentration of 0.3 mg per disc) were also used. The CDT-KPC test was performed using the recommended by EUCAST reference strain *K. pneumoniae* ATCC BAA-1705. In the case of PBA, the standard KPC inhibitor, a difference of at least 4 mm in the inhibition zone of MEM-PBA versus MEM-10 for *K. pneumoniae* ATCC BAA-1705 should be obtained [52]. The KPC carbapenemases inhibitor activity of new tested agents was evaluated by comparison of the diameter of inhibition zone around the disc with meropenem supplemented with a new agent to the diameter of inhibition zone around the disc with meropenem alone. In this study, we assumed that if the new compound has BLI activity then the difference in these diameters should also be at least 4 mm;

(2) CDT-AmpC is the modified phenotypic test previously described by Yagi et al. [51] for detection class C β-lactamase-producing *Enterobacteriaceae* by using 3-aminophenylboronic acid (APB). This test has been specially modified for the purpose of this

work in order to meet general procedures for detection of resistance mechanisms recommended by EUCAST [52]. The CDT-AmpC test was performed using two AmpC-producing clinical isolates: *P. aeruginosa* MUW 700 with overexpression of chromosomally encoded cephalosporinase AmpC and *E. coli* 77 with plasmid-acquired AmpC cephalosporinase CMY-2. The AmpC cephalosporinases inhibitor activity of new tested agents was evaluated by comparison of the diameter of inhibition zone around the disc with ceftazidime (CAZ-30) supplemented with a new agent (0.3 mg per disc) to the diameter of inhibition zone around the disc with ceftazidime alone. PBA at the concentration of 0.3 mg per disc was used as the reference BLI which is known to inhibit the activity of both KPC [52] and AmpC enzymes [53]. The results of BLI activity were evaluated after incubation at 35 ^{o}C for 18 hours. It was assumed in this study that, in the presence of reference compound PBA and new agents with BLI activity, a difference of at least 5 mm in the inhibition zones around the disc with CAZ-PBA or CAZ+new agent versus CAZ-30 in the case of *P. aeruginosa* MUW 700 as well as *E. coli* 77 should be observed. Ceftazidime was chosen for this study also following Xia et al. [54] who observed increased susceptibility of AmpC-producing strains to this cephalosporin in the presence of some new benzoxaboroles as β-lactamase inhibitors;

(3) CDT-ESBL is the EUCAST phenotypic test using disc with ceftazidime (CAZ-30) or cefotaxime (CTX-30) alone and disc with this β-lactam supplemented with clavulanic acid (CAZ-CL and CTX-CL) (Becton Dickinson) in concentration 0.01 mg per disc. The ESBL inhibitor activity of new tested agents was evaluated by comparison of the diameter of inhibition zone around the disc with ceftazidime and cefotaxime supplemented with a new agent (0.3 mg per disc) to the diameter of inhibition zone around the disc with β-lactam alone. In the case of clavulanic acid, the standard ESBL inhibitor, a difference of at least 5 mm in the inhibition zone of CAZ-CL versus CAZ-30 and CTX-CL versus CTX-30 for *K. pneumoniae* ATCC 700603 should be obtained [52]. Using the new compounds as BLI, we assumed that the difference in these diameters should also be at least 5 mm.

Microdilution test for detection of BLI activity. The ability of new studied agents to inhibit the activity of various classes of carbapenemases, AmpC-type and ESBL enzymes was examined by the MIC values of β-lactam determination assays, with or without benzosiloxaboroles, according to the CLSI [68] recommendations. Ceftazidime was used to determine the BLI activity against various classes of β-lactamases, While meropenem allowed the analyzes of new agent activity only against carbapenemases. All studied benzosiloxaboroles and PBA were added at a the concentration of 0.016 mg/L. The MIC

determination was performed in Mueller-Hinton II broth medium (MHB) (Becton Dickinson). Results of BLI activity were evaluated after incubation at 35 ^{o}C for 18 hours. It was assumed that at least a 4-fold decrease in the MIC value of β-lactams after the addition of PBA and new agent with BLI activity should be observed.

Cytotoxic studies. (1) Culture method. MRC-5 pd30 human fibroblasts were cultured in MEM (Gibco) supplemented with 10% fetal bovine serum (EuroClone), 2mM L-glutamine, antibiotics (100 U/ml penicillin, 100 μg/ml streptomycin, Sigma-Aldrich) and 1% non-essential amino-acids (Sigma-Aldrich). Cells were grown in 75 cm^2 cell culture flasks (Sarstedt), in a humidified atmosphere of CO_2/air (5/95%) at 37˚C.

MTT-based viability assay

(2) MTT-based viability assay. Stock solutions of the tested compounds were prepared in DMSO, so the final concentration of vehicle was 0.5% in each case. For cytotoxicity studies 2-fold serial dilutions were prepared in the proper medium containing 0.5% DMSO. All the experiments were performed in exponentially growing cultures. Before treatment MRC-5 cells were trypsinized in 0.25% trypsin-EDTA solution (Sigma-Aldrich) and seeded into 96-well microplates (Sarstedt) at a density of 8×10^3 cells/well. Cells were treated with the tested compounds or DMSO (0.5%) at the appropriate concentrations 18 h after plating. After 72h incubation with the compounds, the supernatants were discarded, and subsequently MTT stock solution (Sigma-Aldrich) was added to each well to the final concentration of 1 mg/ml. After 1 h incubation at 37˚C, water-insoluble dark blue formazan crystals were dissolved in DMSO (100 μl) (37˚C/10 min incubation). Optical densities were measured at 570 nm using BioTek microplate reader. All measurements were carried out in four replicates and the results expressed as a percent of viable cells versus control cells.

Docking and molecular dynamics

Three most promising compounds (**10, 27, 37** and 4-FBOB) were modeled with semi-flexible molecular docking approach. The search of PDB database for boron-compoundcontaining β-lactamase structures revealed that all systems are covalently bonded to the serine residue in a pocket. Furthermore, organoboron molecules are present in their anionic form with tetracoordinate boron atom. In the current studies all possible ionized forms of the compounds were thus generated and docked using MOE2016.08 [71] to the KPC-2 β-lactamase structure derived from PDB (ID: 3RXX) [64]. The geometry binding pocket was minimized in the absence of a compound. Scoring function GBVI/WSA dG was applied. Results, where boron atom was placed closer than 4 Å to Ser70 sidechain oxygen atom, were qualified as potent to form a covalent bond. Only those results were retained and B-O-Ser70 bod was introduced

into each mode. Following the water molecule and counterions placement, a careful energy minimalization and thermalization was performed. Molecular dynamics (2 ns) was run in a rectangular cuboid periodic box at 300 K using Nosé–Poincaré algorithm [72,73]. In addition, molecular dynamics of non-covalently bound systems as well as free compounds in water were carried out in the same conditions. Each system was simulated in three independent repetitions. AMBER10:EHT forcefield was applied in all calculations [74,75]. Structural and energetic analysis were performed for each run. The compound-protein and compound-solvent interactions were investigated using MOE Ligand Interactions tool [71]. Energy of covalently bonded and non-bonded systems throughout dynamics simulations were compared for each mode and compounds were arranged in interaction energy-based order. Covalently bound 3-NO_2-PBA interactions from 3RXX structure [64], were used as a reference in binding analysis as this compound is the most similar to the well-studied PBA (it possesses aromatic ring and proven inhibitory properties). KPC-3 amino acid sequence derived from Q93DC4 Uniprot accession number [76] was used for comparison with KPC-2.

Acknowledgements

This work was supported by Warsaw University of Technology. Research on antimicrobial activity was carried out with the use of CePT infrastructure financed by the European Union - the European Regional Development Fund within the Operational Programme “Innovative economy” for 2007–2013. Moreover, the microbiology study was supported by the Foundation for the Development of Diagnostics and Therapy, Warsaw, Poland (REGON: 006220910, NIP: 5262173856, KRS: 0000195643). The authors are grateful to Prof. Marek Gniadkowski for providing standard, clinical and transformant strains producing KPC-type and CMY-2 enzymes. Dr Patrycja Wińska is thanked for performing cytotoxicity studies. Molecular modelling studies were supported by Faculty of Physics, University of Warsaw (BST-176600/BF/22). Computations were carried out using infrastructures financed by POIG.02.01.00-14-122/09.

Accession Codes. Compounds **10**, **27**, **37**: PDB ID 3RXX. Authors will release the atomic coordinates and experimental data upon article publication.

List of abbreviations

ESBL – extended spectrum β-lactamase

BDEA – *N*-butyldiethanolamine

BLI - β-lactamase inhibitor

CAZ - ceftazidime

CDT - combination disc test

CLSI - Clinical and Laboratory Standards Institute

CTX - cefotaxime

EUCAST - European Committee on Antimicrobial Susceptibility Testing

FL - fluconazole

4FBOB – 4-fluorobenzoxaborole

KPC - *Klebsiella pneumoniae* carbapenemase

LTMP – lithium 2,2,6,6-tetramethylpiperidide

MBC – minimum bactericidal concentration

MD – molecular dynamics

MDR – multidrug resistant

MEM – meropenem

MHA - Müller-Hinton agar

MIC – minimum inhibitory concentration

3-NPBA – 3-nitrophenylboronic acid

PAβN - phenylalanine-arginine β-naphthylamide

PBA – phenylboronic acid

PDB – protein data base

SAR – structure activity relationship

TSA – tryptic soy agar

References

[1] K. Torssell, Zur Kenntnis der Arylborsäuren 0.3, Bromierung der Tolylborsäuren nach Wohl-Ziegler, Arkiv Kemi 10 (1957) 507−511.

[2] S.J. Baker, Y.K. Zhang, T. Akama, A. Lau, H. Zhou, V. Hernandez, W. Mao, M.R.K. Alley, V. Sanders, J.J. Plattner, Discovery of a new boron-containing antifungal agent, 5-fluoro-1,3-dihydro-1-hydroxy-2,1-benzoxaborole (AN2690), for the potential treatment of onychomycosis, J. Med. Chem. 49 (2006) 4447–4450.

[3] F.L. Rock, W. Mao, A. Yaremchuk, M. Tukalo, T. Crepin, H.C. Zhou, Y.K. Zhang, V. Hernandez, T. Akama, S.J. Baker, J.J. Plattner, L. Shapiro, S.A. Martinis, S.J. Benkovic, S.

Cusack, M.R.K. Alley, An antifungal agent inhibits an aminoacyl-tRNA synthetase by trapping tRNA in the editing site, Science 316 (2007) 1759–1761.

[4] T. Akama, S.J. Baker, Y.K. Zhang, V. Hernandez, H. Zhou, V. Sanders, Y. Freund, R. Kimura, K.R. Maples, J. Plattner, Discovery and structure-activity study of a novel benzoxaborole anti-inflammatory agent (AN2728) for the potential topical treatment of psoriasis and atopic dermatitis, Bioorg. Med. Chem. Lett. 19 (2009) 2129–2132.

[5] Y.R. Freund, T. Akama, M.R.K. Alley, J. Antunes, C. Dong, K. Jarnagin, R. Kimura, J.A. Nieman, K.R. Maples, J.J. Plattner, F. Rock, R. Sharma, R. Singh, V. Sanders, Y. Zhou, Boron-based phosphodiesterase inhibitors show novel binding of boron to PDE4 bimetal center, FEBS Lett. 586 (2012) 3410–3414.

[6] E. Seiradake, W. Mao, V. Hernandez, S.J. Baker, J.J. Plattner, M.R.K. Alley, S. Cusack, Crystal structures of the human and fungal cytosolic Leucyl-tRNA synthetase editing domains: A structural basis for the rational design of antifungal benzoxaboroles, J. Mol. Biol. 390 (2009) 196–207.

[7] H.Y. Li, H.Y. Wang, Y.C. Liu, Z. Liu, A benzoboroxole-functionalized monolithic column for the selective enrichment and separation of cis-diol containing biomolecules, Chem. Commun. 48 (2012) 4115–4117.

[8] R.E. Mendes, M.R. Alley, H.S. Sader, D.J. Biedenbach, R.N. Jones, Potency and spectrum of activity of AN3365, a novel boron-containing protein synthesis inhibitor, tested against clinical isolates of *Enterobacteriaceae* and nonfermentative Gram-negative bacilli, Antimicrob. Agents Chemother. 57 (2013) 2849–2857.

[9] Anacor Pharmaceuticals. FDA approves Anacor Pharmaceuticals' KERYDIN™ (Tavaborole) topical solution, 5% for the treatment of onychomycosis of the toenails, press release, July 8, 2014. http:// investor.anacor.com/.

[10] N. Sharma, D. Sharma, An upcoming drug for onychomycosis: Tavaborole, J. Pharmacol. Pharmacother. 6 (2015) 236-239.

[11] Anacor Pharmaceuticals. FDA approves Anacor Pharmaceuticals' CRISABOROLE, December 14, 2016. http:// investor.anacor.com/.

[12] M.P. Anthony, J.N. Burrows, S. Duparc, J.J. Moehrle, T.N. Wells, The global pipeline of new medicines for the control and elimination of malaria, Malar. J. 11 (2012) 316-322.

[13] Z.T. Qiao, Q. Wang, F.L. Zhang, Z.L. Wang, T. Bowling, B. Nare, R.T. Jacobs, J. Zhang, D.Z. Ding, Y.G. Liu, H.C. Zhou, Chalcone-benzoxaborole hybrid molecules as potent antitrypanosomal agents, J. Med. Chem. 55 (2012) 3553−3557.

[14] X.F. Li, S.M. Zhang, Y.K. Zhang, Y.D. Liu, C.Z. Ding, Y. Zhou, J.J. Plattner, S.J. Baker, W. Bu, L. Liu, W.M. Kaźmierski, M.S. Duan, R.M. Grimes, L.L. Wright, G.K. Smith, R.L. Jarvest, J.J. Ji, J.P. Cooper, M.D. Tallant, R.M. Crosby, K. Creech, Z. Ni, W.X. Zou, J. Wright, Synthesis and SAR of acyclic HCV NS3 protease inhibitors with novel P4-benzoxaborole moieties, Bioorg. Med. Chem. Lett. 21 (2011) 2048–2054.

[15] A. Brzozowska, P. Ćwik, K. Durka, T. Kliś, A.E. Laudy, S. Luliński, J. Serwatowski, S. Tyski, M. Urban, W. Wróblewski, Benzosiloxaboroles: silicon benzoxaborole congeners with improved Lewis acidity, high diol affinity, and potent bioactivity, Organometallics 34 (2015) 2924–2932.

[16] A.J. Bridges, A. Lee, E.C. Maduakor, C.E. Schwartz, Fluorine as an ortho-directing group in aromatic metalation: Generality of the reaction and the high position of fluorine in the Dir-Met potency scale, Tetrahedron Lett. 33 (1992) 7495–7498.

[17] A.J. Bridges, A. Lee, E.C. Maduakor, C.E. Schwartz, Fluorine as an ortho-directing group in aromatic metalation: A two-step preparation of substituted benzo(b)thiophene-2-carboxylates, Tetrahedron Lett. 33 (1992) 7499–7502.

[18] F. Mongin, O. Desponds, M. Schlosser, Reagent-modulated optional site selectivities: The metalation of *o*-, *m*- and *p*-halobenzotrifluorides, Tetrahedron Lett. 37 (1996) 2767–2770.

[19] W. Yang, J. Zhou, B. Wang, H. Ren, Lewis acid-promoted synthesis of unsymmetrical and highly functionalized carbazoles and dibenzofurans from biaryl triazenes: application for the total synthesis of clausine C, clausine R, and clauraila A, Chem. Eur. J. 17 (2011) 13665–13669.

[20] M.M. Heravi, N. Abdolhosseini, H.A. Oskooie, Regioselective and high-yielding bromination of aromatic compounds using hexamethylenetetramine–bromine, Tetrahedron Lett. 46 (2005) 8959–8963.

[21] T. Kunz, P. Knochel, Synthesis of functionalized benzo(*b*)thiophenes by the intramolecular copper-catalyzed carbomagnesiation of alkynyl(aryl)thioethers, Angew. Chem. Int. Ed. 51 (2012) 1958–1961.

[22] T. Jensen, H. Pedersen, B. Bang-Andersen, R. Madsen, M. Joergensen, Palladium-catalyzed aryl amination–heck cyclization cascade: a one-flask approach to 3-substituted indoles, Angew. Chem. Int. Ed. 47 (2008) 888–890.

[23] W. Li, D.P. Nelson, M.S. Jensen, R.S. Hoerrner, D. Cai, R.D. Larsen, P.J. Reider, An improved protocol for the preparation of 3-pyridyl- and some arylboronic acids, J. Org. Chem. 67 (2002) 5394-5397.

[24] K. Durka, S. Luliński, J. Smętek, M. Dąbrowski, J. Serwatowski, K. Woźniak, The influence of boronate groups on the selectivity of the Br–Li exchange in model dibromoaryl boronates, Eur. J. Org. Chem. 15 (2013) 3023–3032.

[25] M. Czub, K. Durka, S. Luliński, J. Łosiewicz, J. Serwatowski, M. Urban, K. Woźniak, Synthesis and transformations of functionalized benzosiloxaboroles, Eur. J. Org. Chem. 4 (2017) 818–826.

[26] J.W. Tomsho, A. Pal, D.G. Hall, S.J. Benkovic, Ring structure and aromatic substituent effects on the pK_a of the benzoxaborole pharmacophore, ACS Med. Chem. Lett. 3 (2012) 48−52.

[27] M.A. Pfaller, D.J. Diekema, Epidemiology of invasive candidiasis: a persistent public health problem, Clin. Microbiol. Rev. 20 (2007) 133-163.

[28] Clinical and Laboratory Standards Institute (CLSI), Method for Antifungal Disk Diffusion Susceptibility Testing of Yeasts, Document M44-A2, 2nd ed., CLSI, 940 West Valley Road, Wayne, Pennsylvania, USA, 2009.

[29] Clinical and Laboratory Standards Institute (CLSI), Reference Method for Broth Dilution Antifungal Susceptibility Testing of Yeasts, Document M27A3, 3rd ed., CLSI, 940 West Valley Road, Wayne, Pennsylvania, USA, 2008.

[30] European Committee on Antimicrobial Susceptibility Testing (EUCAST), Method for the determination of broth dilution MIC of antifungal agents for yeasts, Document E.DEF 7.3.1, 2017 (accessed 15.01.2017). http://www.eucast.org/.

[31] J. Gong, M. Xiao, H. Wang, T. Kudinha, Y. Wang, F. Zhao, W. Wu, L. He, Y.-C. Xu, J. Zhang, Genetic Differentiation, Diversity, and Drug Susceptibility of *Candida krusei*, Front. Microbiol. 9: 2717 (2018) doi: 10.3389/fmicb.2018.02717.

[32] M.A. Pfaller M. Bale, B. Buschelman M. Lancaster, A. Espinel-Ingroff, J.H. Rex, M.G. Rinaldi. Selection of candidate quality control isolates and tentative quality control ranges for in vitro susceptibility testing of yeast isolates by National Committee for Clinical Laboratory Standards proposed standard methods, J. Clin. Microbiol. 32 (1994), 1650-1653.

[33] ETEST Application guide, BioMerieux. http://www.biomerieux-usa.com/clinical/etest.

[34] ETEST for antifungal susceptibility testing – research gate, AB BIODISK. https://www.researchgate.net/...fungal.../Etest.pdf

[35] V. Hernandez, T. Crépin, A. Palencia, S. Cusack, T. Akama, S.J. Baker, W. Bu, L. Feng, Y.R. Freund, L. Liu, M. Meewan, M. Mohan, W. Mao, F.L. Rock, H. Sexton, A. Sheoran, Y. Zhang, Y.K. Zhang, Y. Zhou, J.A. Nieman, M.R. Anugula, E.M. Keramane, K. Savariraj, D.S. Reddy, R. Sharma, R. Subedi, R. Singh, A. O'Leary, N.L. Simon, P.L. De Marsh, S.

Mushtaq, M. Warner, D.M. Livermore, M.R. Alley, J.J. Plattner, Discovery of a novel class of boron-based antibacterials with activity against Gram-negative bacteria, Antimicrob. Agents Chemother. 57 (2013) 1394-1403.

[36] J.E. Ross, N. Scangarella-Oman, R.N. Jones, Determination of disk diffusion and MIC quality control guidelines for GSK2251052: a novel boron-containing antibacterial, Diagn. Microbiol. Infect. Dis. 75 (2013) 437-439.

[37] K. O'Dwyer, A.T. Spivak, K. Ingraham, S. Min, D. J. Holmes, C. Jakielaszek, S. Rittenhouse, A.L. Kwan, G.P. Livi, G. Sathe, E. Thomas, S. Van Horn, L.A. Miller, M. Twynholm, J. Tomayko, M. Dalessandro, M. Caltabiano, N.E. Scangarella-Oman, J.R. Brown, Bacterial resistance to leucyl-tRNA synthetase inhibitor GSK2251052 develops during treatment of complicated urinary tract infections, Antimicrob. Agents Chemother. 59 (2015) 289-298.

[38] European Committee on Antimicrobial Susceptibility Testing (EUCAST). Breakpoint tables for interpretation of MICs and zone diameters. Version 8.0, 2018 (valid 01.01.2018). http://www.eucast.org/

[39] Clinical and Laboratory Standards Institute (CLSI), Performance standards for antimicrobial susceptibility testing. Document CLSI supplement M100, 28th ed., January 2018. 950 West Valley Road, Wayne, Pennsylvania, USA, 2018.

[40] K.P. Purnapatre, M. Rao, M. Pandya, A. Khanna, T. Chaira, R. Bambal, D.J. Upadhyay, N. Masuda, *In vitro* and *in vivo* activities of DS86760016, a novel leucyl-tRNA synthetase inhibitor for Gram-negative pathogens, Antimicrob. Agents Chemother. 62 (2018) e01987-17. https://doi.org/10.1128/AAC.01987-17.

[41] J.M.A. Blair, G.E. Richmond, L.J.V. Piddock, Multidrug efflux pumps in Gram-negative bacteria and their role in antibiotic resistance, Future Microbiol. 9 (2014) 1165–1177.

[42] A.E. Laudy, A. Mrowka, J. Krajewska, S. Tyski, The influence of efflux pump inhibitors on the activity of non-antibiotic NSAIDS against Gram-negative rods, PLoS One 11 (2016) e0147131. https://doi:10.1371/journal.pone.0147131.

[43] A.E. Laudy, E. Kulińska, S. Tyski, The impact of efflux pump inhibitors on the activity of selected non-antibiotic medicinal products against Gram-negative bacteria, Molecules 22 (2017) pii: E114. https://doi:10.3390/molecules22010114.

[44] X.Z. Li, P. Plesiat, H. Nikaido, The challenge of efflux-mediated antibiotic resistance in Gram-negative bacteria, Clin. Microbiol. Rev. 28 (2015) 337–418.

[45] J.M. Pagès, L. Amaral, Mechanisms of drug efflux and strategies to combat them: Challenging the efflux pump of Gram-negative bacteria, Biochim. Biophys. Acta 1794 (2009) 826–833.

[46] U.O. Hasdemir, J. Chevalier, P. Nordmann, J.M. Pagès, Detection and prevalence of active drug efflux mechanism in various multidrug resistant *Klebsiella pneumoniae* strains from Turkey, J. Clin. Microbiol. 42 (2004) 2701–2706.

[47] B. Zechini, I. Versace, Inhibitors of multidrug resistant efflux systems in bacteria, Recent Pat. Antiinfect. Drug Discov. 4 (2009) 37–50.

[48] M. Malléa, J. Chevalier, A. Eyraud, J. M. Pagès, Inhibitors of antibiotic efflux pump in resistant *Enterobacter aerogenes* strains, Biochem. Biophys. Res. Commun. 293 (2002) 1370–1373.

[49] S. Baucheron, H. Imberechts, E. Chaslus-Dancla, A. Cloeckaert, The AcrB multidrug transporter plays a major role in high-level fluorquinolone resistance in *Salmonella enterica* serovar Thyphimurium phage typer DT 204, Microb. Drug Resist. 8 (2008) 281–289.

[50] P. A. Kiener, S. G. Waley, Reversible inhibitors of penicillinases, Biochem. J. 169 (1978) 197-204.

[51] K. Bush, A resurgence of β-lactamase inhibitor combinations effective against multidrug-resistant Gram-negative pathogens, Int. J. Antimicrob. Agents 46 (2015) 483-493.

[52] European Committee on Antimicrobial Susceptibility Testing (EUCAST), EUCAST guidelines for detection of resistance mechanisms and specific resistance of clinical and/or epidemiological importance, Document version 1.0, 2013 (accessed 11.12.2013). http://www.eucast.org/.

[53] T. Yagi, J. Wachino, H. Kurokawa, S. Suzuki, K. Yamane, Y. Doi, N. Shibata, H. Kato, K. Shibayama, Y. Arakawa, Practical methods using boronic acid compounds for identification of class C β-lactamase-producing *Klebsiella pneumoniae* and *Escherichia coli*, J. Clin. Microbiol. 43 (2005) 2551-2558.

[54] Y. Xia, K. Cao, Y. Zhou, M.R. Alley, F. Rock, M. Mohan, M. Meewan, S.J. Baker, S. Lux, C.Z. Ding, G. Jia, M. Kully, J.J. Plattner, Synthesis and SAR of novel benzoxaboroles as a new class of β-lactamase inhibitors, Bioorg. Med. Chem. Lett. 21 (2011) 2533-2536.

[55] S.C.J. Jorgensen, M.J. Rybak, Meropenem and vaborbactam: stepping up the battle against carbapenem-resistant *Enterobacteriaceae*, Pharmacother. 38 (2018) 444-461.

[56] Drug leaflet, VABOMERE (meropenem and vaborbactam) for injection – FDA. https://www.accessdata.fda.gov/drugsatfda_docs/label/2017/209776lbl.pdf

[57] O. Lomovskaya, D. Sun, D. Rubio-Aparicio, K. Nelson, R. Tsivkovski, D.C. Griffith, M.N. Dudley, Vaborbactam: spectrum of β-lactamase inhibition and impact of resistance mechanisms on activity in *Enterobacteriaceae*, Antimicrob. Agents. Chemother. 61 (2017) e01443-17. https://doi.org/10.1128/AAC.01443-17.

[58] M.A. Hackel, O. Lomovskaya, M.N. Dudley, J.A. Karlowsky, D.F. Sahm, *In vitro* activity of meropenem-vaborbactam against clinical isolates of KPC-positive *Enterobacteriaceae*, Antimicrob. Agents. Chemother. 62 (2018) e01904-17. https://doi.org/10.1128/AAC.01904-17.

[59] J.D. Docquier, S. Mangani, An update on β-lactamase inhibitor discovery and development, Drug Res. Updates 36 (2018) 13-29.

[60] E. Munson, M.D. Huband, M. Castanheira, K.A. Fedler, R.K. Flamm, Determination of MIC and disk diffusion quality control guidelines for meropenem-vaborbactam, a novel carbapenem/boronic acid β-lactamase inhibitor combination, Diagn. Microbiol. Infect. Dis. 90 (2018) 324-328.

[61] Available at https://www.ncbi.nlm.nih.gov/genbank/

[62] N. Stoesser, A.E. Sheppard, G. Peirano, L.W. Anson, L. Pankhurst, R. Sebra, H.T.T. Phan, A. Kasarskis, A.J. Mathers, T.E.A. Peto, P. Bradford, M.R. Motyl, A.S. Walker, D.W. Crook, J.D. Pitout, Genomic epidemiology of global *Klebsiella pneumoniae* carbapenemase (KPC)-producing *Escherichia coli*, Sci Rep. (2017) 7:5917. https://doi:10.1038/s41598-017-06256-2.

[63] L.S. Munoz-Price, L. Poirel, R.A. Bonomo, M.J. Schwaber, G.L. Daikos, M. Cormican, G. Cornaglia, J. Garau, M. Gniadkowski, M.K. Hayden, K. Kumarasamy, D.M. Livermore, J.J. Maya, P. Nordmann, J.B. Patel, D.L. Paterson, J. Pitout, M.V. Villegas, H. Wang, N. Woodford, J.P. Quinn, Clinical epidemiology of the global expansion of *Klebsiella pneumoniae* carbapenemases, Lancet Infect. Dis. 13 (2013) 785–796.

[64] W. Ke, C.R. Bethel, K.M. Papp-Wallace, S.R.R. Pagadala, M. Nottingham, D. Fernandez, J.D. Buynak, R.A. Bonomo, F. van den Akker, Crystal structures of KPC-2 β-lactamase in complex with 3-nitrophenyl boronic acid and the penam sulfone PSR-3-226, Antimicrob. Agents Chemother. 56 (2012) 2713–2718.

[65] K. Bush, J.F. Fisher, Epidemiological expansion, structural studies, and clinical challenges of new β-lactamases from Gram-negative bacteria, Annu. Rev. Microbiol. 65 (2011) 455-478.

[66] W.H. Sheng, R.E. Badal, P.R. Hsueh, SMART Program, Distribution of extended-spectrum β-lactamases, AmpC β-lactamases, and carbapenemases among *Enterobacteriaceae* isolates causing intra-abdominal infections in the Asia-Pacific region: results of the study for Monitoring Antimicrobial Resistance Trends (SMART), Antimicrob. Agents Chemother. 57 (2013) 2981–2988.

[67] European Committee on Antimicrobial Susceptibility Testing (EUCAST), Disk diffusion method for antimicrobial susceptibility testing, Document version 6.0, 2017 (accessed 9.01.2017). http://www.eucast.org/.

[68] Clinical and Laboratory Standards Institute (CLSI), Methods for dilution antimicrobial susceptibility tests for bacteria that grow aerobically, Approved Standard, Document M07-A9, 9th ed., CLSI, 940 West Valley Road, Wayne, Pennsylvania, USA, 2012.

[69] Clinical and Laboratory Standards Institute (CLSI), Methods for determining bactericidal activity of antimicrobial agents, Approved Guideline, Document M26-A. CLSI, 940 West Valley Road, Wayne, Pennsylvania, USA, 1999.

[70] R.P. Lamers, J.F. Cavallari, L.L. Burrows, The efflux inhibitor phenylalanine-arginine β-naphthylamide (PAβN) permeabilizes the outer membrane of Gram-negative bacteria, PLoS One 8 (2013) e60666. https://doi.org/10.1371/journal.pone.0060666

[71] Molecular Operating Environment (MOE), 2016.08; Chemical Computing Group Inc., 1010 Sherbrooke St. West, Suite #910, Montreal, QC, Canada, H3A 2R7, 2016.

[72] J.B. Sturgeon, B.B. Laird, Symplectic algorithm for constant pressure molecular dynamics using a Nosé-Poincaré Thermostat; University of Kansas Technical Paper, 2002.

[73] S.D. Bond, J.L. Benedict, B.B. Laird, The Nosé-Poincaré method for constant temperature molecular dynamics, J. Comp. Phys. 151 (1999) 114–134.

[74] D.A. Case, T.A. Darden, T.E. Cheatham, III, C.L. Simmerling, J.Wang, R.E. Duke, R. Luo, M. Crowley, R.C. Walker, W. Zhang, K. M. Merz, B. Wang, S. Hayik, A. Roitberg, G. Seabra, I. Kolossváry, K.F. Wong, F.Paesani, J. Vanicek, X. Wu, S.R. Brozell, T. Steinbrecher, H. Gohlke, L. Yang, C. Tan, J. Mongan, V. Hornak, G. Cui, D. H. Mathews, M.G. Seetin, C. Sagui, V. Babin, P.A. Kollman, AMBER 10, University of California, San Francisco, 2008.

[75] P.R. Gerber , K. Müller, MAB, a generally applicable molecular force field for structure modelling in medicinal chemistry, J. Comput. Aided Mol. Des. 9 (1995) 251–268.

[76] S. Pundir, M.J. Martin, C. O'Donovan, UniProt Protein Knowledgebase, Methods Mol. Biol. 1558 (2017) 41–55.

- Synthesis and characterization of a series of 22 functionalized benzosiloxaboroles
- Strong antifungal activity of fluorinated derivatives
- KPC/AmpC inhibitory activity of selected benzosiloxaboroles
- Docking and molecular dynamics studies on the binding to the KPC-2 β-lactamase